CHALMERS
UNIVERSITY OF TECHNOLOGY

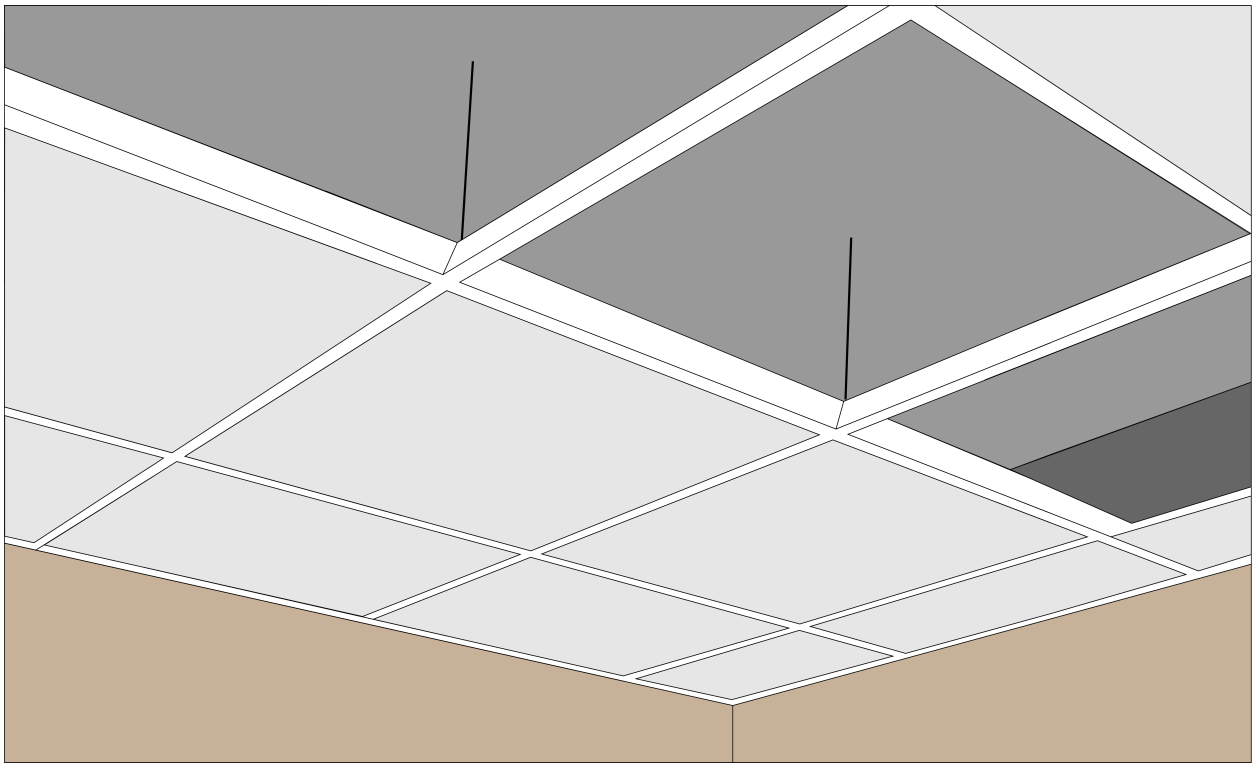

# Investigation of the Predictability of Porous Ceiling Absorbers with Large Cavities

Master's thesis in Sound and Vibration

JOHANNA JONASSON

DEPARTMENT OF ARCHITECTURE AND CIVIL ENGINEERING
CHALMERS UNIVERSITY OF TECHNOLOGY
Gothenburg, Sweden 2024
www.chalmers.se

Master's thesis 2024

# Investigation of the Predictability of Porous Ceiling Absorbers with Large Cavities

JOHANNA JONASSON


CHALMERS
UNIVERSITY OF TECHNOLOGY

Department of Architecture and Civil Engineering
*Division of Applied Acoustics*
Chalmers University of Technology
Gothenburg, Sweden 2024

Investigation of the Predictability of Ceiling Absorbers with Large Cavities
JOHANNA JONASSON



Supervisor: Robin Thomas Helland, Brekke & Strand Akustikk
Examiner: Jens Forssén, Division of Applied Acoustics

Master's Thesis 2024
Department of Architecture and Civil Engineering
Division of Applied Acoustics
Chalmers University of Technology
SE-412 96 Gothenburg
Telephone +46 31 772 1000

Cover: An illustration of a suspended ceiling with several tiles missing. Illustrated by Johanna Jonasson.

Typeset in LaTeX
Printed by Chalmers Reproservice
Gothenburg, Sweden 2024

Investigation of the Predictability of Porous Ceiling Absorbers with Large Cavities

JOHANNA JONASSON
Department of Architecture and Civil Engineering
Division of Applied Acoustics
Chalmers University of Technology

# Abstract

Modern construction often accommodates large installations, leading to unwanted large air cavities between the acoustic ceiling and floor structure. This raises concerns about the absorption coefficient of the porous absorbers and its impact on room acoustics. Porous ceiling absorber suppliers typically do not provide data for cavities larger than 400 mm, leading to potential inaccuracies in predicted reverberation times and challenges in achieving optimal acoustic environments.

This study investigates the impact of large cavities above porous ceiling absorbers by creating a model based on the transfer matrix model and Delany-Bazley's impedance prediction method. The model is developed to predict the absorption coefficient of acoustic ceilings, and its accuracy is validated through measurements and software simulations.

Even if the model is limited to calculating infinite areas and only using Daleny-Bazley's impedance model, which is not the most accurate, the results show problems for the absorption coefficient with variation in the cavities and the airflow resistivity. The results show that porous absorbers have a higher absorption at higher frequencies and that an air gap increases the overall absorption but has a minimal influence at high frequencies. However, increasing the absorber's thickness or airflow resistivity does not always result in better absorption, especially with large air cavities. In cases with high airflow resistivity, the absorption at low frequencies can even decrease.

The thesis also discusses the edge effect that occurs in reverberation room measurement, positive and negative influences on the classification of absorbers, and the challenges that building acousticians face. Further measurements and research on mounted ceiling systems are necessary for future work. The model needs to be developed for finite areas and with a more complex impedance prediction method for it to be adapted to real-world scenarios.

Keywords: transfer matrix model, building acoustics, porous ceiling absorbers, absorption coefficient

# Acknowledgements

I would like to express my deepest gratitude to my examiner, Jens Forssén, for his valuable insights and guidance throughout this project. Thank you for always answering all my questions and keeping me on the right path.

A special thanks go to my supervisor, Robin Thomas Helland, for proposing this assignment and for his support and encouragement during the entire process. I would also like to extend my heartfelt appreciation to everyone at Brekke & Strand Akustikk in Oslo for their warm hospitality and assistance during my work.

Finally, to my family, thank you for your unconditional love and support, and belief in me throughout my academic journey.

Johanna Jonasson, Gothenburg, October 2024

# Contents

# 1

# Introduction

In modern construction techniques, the accommodation of various installations often leads to large voids between the ceiling system and the floor structure within new constructions. This trend, that projected to persist into the foreseeable future, has been observed by Brekke & Strand Akusik in Norway and Sweden. As the number of projects adopting similar solutions continues, concerns regarding the impact on room acoustics have come to light.

Suppliers of ceiling absorbers commonly do not provide data for absorption coefficients for air cavities larger than 400 mm. This lack of information can lead to inaccuracies in predicted reverberation times, making it challenging to achieve optimal acoustic environments. Additionally, the methods used to classify and measure ceiling absorbers are often debated due to various uncertainties and limitations [1, 2, 3].

Despite the regular practice of conducting on-site measurements of reverberation time [4, 5], current measurement methods fall short of offering specific details on the acoustic characteristics. The current methods give no insights into the efficiency of ceiling absorbers or precisely pinpointing areas where the absorption coefficient is insufficient. The tube methods [6, 7], and the room method [8], currently used for measuring absorbers, are insufficient for on-site measurements [9].

Given these challenges, the question of the predictability of the ceiling absorber's absorption and acoustical impact is raised. Is it possible to develop a model that can effectively simulate the absorption characteristics of ceiling absorbers with large air cavities? Such a model could be applied to predict reverberation times with greater accuracy, ensuring that spaces are designed to meet optimal acoustic standards from the outset.

By investigating the preductibility of ceiling absorbers with large air caviteies the growing need for reliable tools in the design of modern spaces, where the interplay between architecture, construction, acoustics, and other building installations is becoming increasingly complex. A working simulation model could significantly improve the knowledge of acoustic performance in modern constructions and offer workable ways to reach the intended acoustic results.

## 1.1 Aim

This thesis aims to study the impact of large cavities above porous ceiling absorbers on room acoustic characteristics, focusing on absorption efficiency, critical frequencies, and panel behavior. To achieve this, a model will be developed to simulate these effects and better understand their implications.

## 1.2 Limitations

This study is limited to buildings within Sweden and Norway, focusing exclusively on the standards and recommendations established in the respective countries. Additionally, the research is confined to non-residential buildings, specifically targeting office spaces, healthcare facilities, schools, and preschools where absorbing ceiling systems are commonly employed. Due to constraints in time and budget, experimentation within laboratory environments is not included in this study.

## 1.3 Background

Effective room acoustics are essential for creating a healthy, comfortable, and functional building environment [10]. This section explains room acoustics, its key concepts, and the regulations and standards governing acoustic requirements in Sweden and Norway. These regulations ensure that spaces meet the necessary acoustic criteria to support health, safety, and overall well-being [4, 5]. The focus will mainly be on reverberation time, absorption coefficient, and the verifications of the two countries.

### 1.3.1 Room acoustics

Room acoustics covers both the physical aspects of sound behavior in an enclosed space and the subjective experience of the listeners [11]. Several key concepts are essential to achieve a healthy and satisfactory sound environment.

Reverberation time refers to the time it takes for the sound pressure level to decrease by 60 db [12]. It is a crucial parameter for assessing the acoustic quality of a room [11]. The ideal reverberation time should be optimized to the room's intended purpose, as different activities require different acoustic environments.

All surfaces in a room either reflect or absorb sound, therefore achieving the right balance is crucial to optimize the room's acoustics for its intended use [13]. Hard surfaces like concrete reflect sound, while soft materials like carpets absorb it [14]. It is also essential to scatter sound evenly across the room to avoid areas with too much sound [11]. Areas containing some irregularities, such as bumps or decoration, help to scatter the sound energy in the room [15]. The dimensions and shape of a room also influence how sound waves travel and interact. Irregular shapes reduce standing waves and echoes, improving the acoustics [15].

### 1.3.2 Regulations and requirements for room acoustics in Sweden

Sound requirements for spaces in buildings in Sweden are controlled by two organizations: the Swedish Work Environment Authority (Arbetsmiljöverket) and the Swedish Institutes of Standards (SIS).

The Swedish Work Environment Authority is a regulatory authority, and they have the mandate from the government and the Riksdag to make sure that the laws about the work environment are followed [16]. AFS 2005:16 is a provision that clarifies the Swedish Working Environment Act [16]. In AFS 2005:16 [17] it is stated that a reverberation time around and below 0.8 seconds is an acceptable disturbance but in environments for children, elderly or hearing-impaired the demands for speech intelligibility is higher and the reverberation time should be below 0.5 seconds.

The Swedish Institute for Standards (SIS) is an international organization specializing in national and international standards [18]. The Swedish Standards Council (Sveriges Standardiseringsförbund) is the principal body for all Swedish standardization and is tasked with promoting interest in standardization and the employment of standards [18]. SS 25268:2023, "Building acoustics - Sound requirements for spaces in buildings", is a standard published by SIS [4]. The standard was developed by a committee of experts in the field of building acoustics, including acousticians, engineers, architects, and other relevant professionals [19].

SS 25268:2023 [4] uses basic requirements and extended requirements where the basic requirement is set to meet the requirements from Boverket's building regulations and the Swedish public health authority, and the extended requirements are used when a better sound environment is desired. The table values in SS 25268:2023 are based on the function of the room and not based on the room description. The standard also specifies if the function of the room shifts over time, a balance between the different reverberation time requirements is needed.

The reverberation time in SS 25268:2023 is divided into two requirements; 125 Hz and the arithmetic mean for 250 Hz, 500 Hz, 1 000 Hz, 2 000 Hz, and 4 000 Hz.

The standard also has regulations regarding the ceiling absorber and involves large office landscapes and open spaces for care work. The values can be seen in Table 1.1.

**Table 1.1:** The requirements from SS 25268:2023 for the sound absorption coefficient in the ceiling for different room functions.

| **Room function** | **Example room description** | **125 Hz** | **250 Hz-4000 Hz** |
|---|---|---|---|
| Office work, $\geq$ 5 locations and $<$ 100 m$^2$ | Office landscape | $\alpha = 0.35$ | $\alpha = 0.9$ |
| Office work, $\geq$ 100 m$^2$ | Office landscape | $\alpha = 0.35$ | $\alpha = 0.9$ |
| Open space for healthcare work $<$ 100 m$^2$ | Nursing expedition, Care square | $\alpha = 0.35$ | $\alpha = 0.9$ |
| Open space for healthcare work $\geq$ 100 m$^2$ | Care square | $\alpha = 0.35$ | $\alpha = 0.9$ |

The standard describes that the absorption effect off the furnishers is only

included in the calculations if the tenant or owner has decided how the room should be furnished. If there is no plan for the furnishers, the room acoustics requirements in the table values need to be achieved by floor, walls, and ceiling without furniture. Low frequency sound reflections also affect the digital sound transmission and it's important with good sound absorption at 125 Hz [4].

Measurement of the reverberation time is done according to ISO 3382-2 and the verifications are executed in 5 % of the room covered by the requirements but are done in at least 3 rooms [4]. SS 25268:2023 allows each octave band to exceed each requirement value with 0.1 s but the mean for 250 Hz to 4000 Hz is not acceptable to exceed. If the measured value for a room fails the verification but is cleared by calculations and the workmanship is controlled and correct, then the first action is to add furnishers and another interior with sound absorption to be able to reach the desired reverberation time according to SS 25267:2023.

### 1.3.3 Regulations and requirements for room acoustics in Norway

In Norway, sound requirements for spaces in buildings are regulated by two key organizations: the Norwegian Work Environment Authority (Arbeidstilsynet) and Standards Norway (Standard Norge). These organizations perform similar roles to their counterparts in Sweden.

Arbetstilsynet is the Norwegian government agency focused on the employee's safety and health [20]. The Working Environment Act is one of the laws and regulations instituted by Arbetstilsynet [20]. The Norwegian Working Environment Act does not have any specific laws or regulations regarding the reverberation time. The only reference to building and room acoustics is in one section where it states that the physical working environment factors relating to buildings shall be fully satisfactory concerning the employees' health and welfare [21].

Standards Norway is a Norwegian member of the International Organization for Standardization (ISO) and the European standardization organization (CEN) [22]. NS 8175:2012 " Acoustic conditions in buildings - Sound classification of various types of buildings" is the Norwegian standard concerning sound conditions in buildings and sound classes for various types of buildings. It was developed by a committee of professionals in the fields of acoustics, engineering, architecture, and other related disciplines [22]. Although NS 8175 was updated in 2019, this newer version has not yet been implemented in the Byggtekniska föreskrifter [23]. As a result, NS 8175:2012 continues to be the standard in use for building regulations [24].

NS 8175:2012 [5] uses a classification system from class A to D, allowing the client to decide which sound classification the building aims for. Class C is the most common classification, and classes A and B are used for buildings with higher demands or buildings with environment classifications [25].

The specified limits apply to the room's average reverberation time in each octave

band of 125 Hz, 250 Hz, 500 Hz, 1000 Hz, 2000 Hz, and 4000 Hz, and the given value for 125 Hz may exceed the limit by up to 40 % [5]. The absorption value is based on the surfaces of an unfurnished room [5].

The reverberation time is verified according to ISO 3382-2 for ordinary rooms and ISO 3382-3 for special rooms [5]. The value for 125 Hz may exceed the given value by up to 40 %, and for frequencies from 250 Hz to 4000 Hz, the values may exceed the limit by up to 20 %, provided the overall mean does not exceed the given value [5].

# 2

# Theory

*This chapter provides a deeper understanding and specific details of the studied subject. It begins with the fundamentals of sound absorbers and the calculation of reverberation time, followed by an overview of existing methods for measuring sound absorption. Finally, the transfer matrix method is introduced for advanced acoustic modeling, offering a deeper insight into the methodology used for the simulation model.*

## 2.1 Sound absorbers

Sound absorbers are important in room acoustics to ensure that only a controlled part of sound energy is reflected within a space [11]. Sound absorbers are used for several purposes including adapting the reverberation time to suit the room's intended use, suppressing unwanted reflections that can cause echoes, and reducing the acoustic energy density and sound pressure levels [15]. Incident sound waves interact with the material in three ways: they can be reflected, transmitted through, or absorbed by the material [13]. When sound is absorbed, the sound energy is converted into heat [11]. The absorption of sound and its frequency depend significantly on the material properties [15]. The absorption factor is calculated by taking the absorbed energy divided by the incident energy [11].

### 2.1.1 Types of absorbers

Sound absorbers can be divided into three main groups: Porous absorbers, membrane absorbers and helmholtz absorbers [11]).

A membrane absorber is constructed from a non-porous, lightweight panel (e.g., metal or hardboard) and is placed at a distance from a hard surface [11]. The distance from the wall creates an air cavity that can be filled with porous material [15]. Sound energy is absorbed due to the low surface weight and high internal losses in the membrane plate [11].

An absorber based on the Helmholtz principle is a membrane or perforated panel featuring holes or slits that are placed with an air cavity behind it [11]. The principle is based on a mass-spring system where the air in the holes acts as the mass, and the volume of air in the cavity provides the spring stiffness [11]. By

vibrating at their mass-air resonance frequency, sound energy is absorbed [13]. The resonance frequency can be adjusted by changing the size of the holes or slits and the volume of the air cavity [13]. The absorption can be increased by adding porous materials to the air cavity [15].

The third one is the porous absorber, often made of mineral wool, plastic foam, or fiberglass [13]. They are typically placed directly on a hard surface or with a cavity behind them [11]. The absorption in a porous material occurs due to friction, viscous effects, and thermal losses [13]. Porous absorbers are commonly used as wall panels, ceiling panels, or suspended ceilings [13].

### 2.1.2 The mechanisms and physical function in porous absorbers

Porous absorbers are materials used in acoustics to reduce sound reflections by converting sound energy into heat [13]. They consist of small interconnected pores that allow sound waves to enter and interact with the material. As the sound passes through, friction, viscous effects, and thermal losses occur, dissipating the sound energy [14]. Porous absorbers are particularly effective at absorbing high- and mid-frequency sounds [13].

Two key properties that determine the effectiveness of porous materials in sound absorption are porosity and airflow resistivity. Porosity refers to the proportion of voids or pores in a material relative to its total volume [15]. Porosity refers to the fraction of the volume of voids or pores within a material relative to the total volume [11]. Higher porosity improves sound absorption because more air pockets can interact with sound waves. Pore size, distribution, material thickness, porosity percentage, and density are some of the factors that affect how well porous materials absorb sound [12]. On the other hand, airflow resistivity ($\sigma$) affects how sound waves travel through the material. When sound waves impact a porous material, they induce pressure fluctuations that cause air to flow through the material [12]. Materials with higher porosity typically exhibit lower airflow resistivity, whereas denser materials with smaller pores tend to have higher resistance. With a high airflow resistivity, the wave will meet a surface having a high impedance, and the wave won't pass through the absorber, resulting in a low absorption [12]. Common materials such as fiberglass, mineral wool, and acoustic foam are designed with specific airflow resistivity to optimize their sound absorption properties [11].

Porous absorbers are often limited in their ability to absorb low-frequency sounds due to their thickness [12]. Low-frequency sound waves have long wavelengths, making it difficult for thin materials to interact with and dissipate these waves effectively. By adding an air gap between the rigid wall or ceiling and the porous absorber, the absorption increases due to a number of physical aspects [15]. The air gap behind the porous absorber makes the sound wave encounter both the porous material and the air space, increasing the overall path length and interaction time. This allows the sound wave to pass through the material twice,

absorbing more energy in the process and providing space for longer wavelengths to interact with the absorber.

As mentioned before, absorption occurs through friction. Friction is most efficient at points of higher particle velocity [13]. Near a wall, the particle velocity is close to zero due to sound wave reflection, creating a region of high pressure and low particle motion [12]. By introducing an air gap, the absorber is positioned at a point where the particle velocity is higher, improving absorption efficiency [15]. This can be seen in Figure 2.1, which shows the movement of the particle velocity.

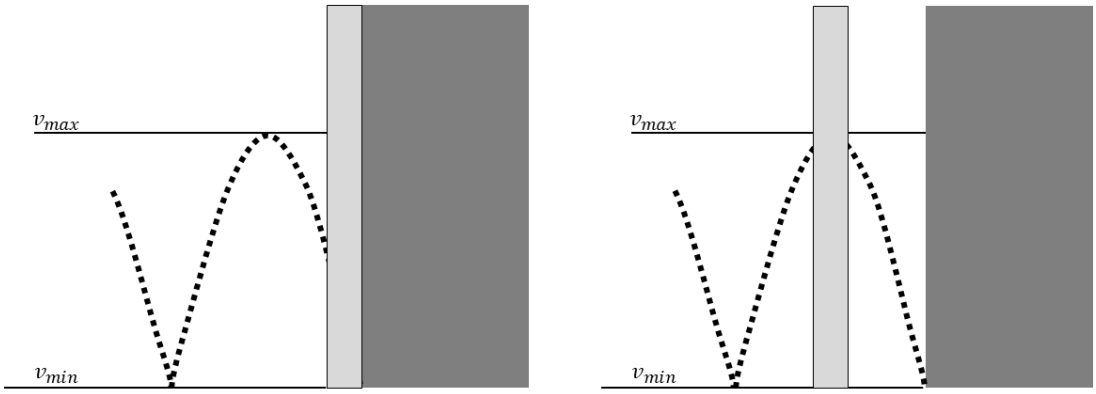


**Figure 2.1:** Illustration of the particle velocity and the impact with an absorber directly mounted on a rigid back or mounded with an air gap.

Placing a thin porous absorber at a quarter, or multiples, of a wavelength from a reflecting surface ensures that it is located where the particle velocity is at its maximum, optimizing sound absorption [13]. In Figure 2.1, the dotted line shows the particles course and its high and low velocity. Contrarily, placing the absorber at multiples of half the wavelength from the surface is less effective due to low particle velocity. To calculate this, the wavelength of sound is given by:

$$\lambda = \frac{v}{f} \tag{2.1}$$

where $\lambda$ is the wavelength (m), $v$ is the speed of sound (m/s), and $f$ is the frequency (Hz) [13].

When the porous absorber is placed at a quarter-wavelength from the surface, it also induces destructive interference, where the reflected sound wave is 180 degrees out of phase with the incoming wave [13]. This phase shift enhances sound absorption at specific frequencies, particularly when the distance through the air gap and back to the absorber equals one-quarter of the wavelength.

### 2.1.3 Absorbers in ceiling panels

Mineral fibers compressed to a stiff board or products using fibers of aluminum compressed into sheets are used as suspended ceilings [11]). Membrane absorbers can be used as absorption in suspended ceilings but then the ceiling is non-porous, solid, or perforated [11]. This thesis will only focus on the porous ceiling systems.

Figure 2.2 shows the type of ceiling system this study is focusing on.

**Figure 2.2:** Picture showing a typical ceiling system installation with suspended porous ceiling absorbers.

As shown in Figure 2.2, the ceiling tiles are mounted in a grid near the walls, leaving no exposed edges. When integrated with ventilation systems, the corresponding tiles are made of metal, which does not provide any sound absorption. One of the tiles in the figure show this case.

## 2.2 Absorption coefficient, absorption area and Sabine's formula

The absorption coefficient is an indicator of the acoustic quality of a material [12]. The absorption coefficient $\alpha$ is defined by

$$\alpha = \frac{W_{abs}}{W_{inc}} \tag{2.2}$$

where $W_{inc}$ is the incident sound power and $W_{abs}$ is the sound power removed from the sound field by the absorbent [12].

Sabine's formula is a key equation in room acoustics used to estimate the reverberation time $T$ (s) of a room [15]. The formula is expressed as

$$T = \frac{55.3}{c_0} \cdot \frac{V}{A} \tag{2.3}$$

where $V$ is the room's volume ($m^3$), $c_0$ is the is the speed of sound in air (m/s) and $A$ represents the equivalent absorption area ($m^2$) [11]. The equivalent absorption area is calculated by summing the products of the absorption coefficient $\alpha_i$ and the surface area $S_i$ ($m^2$) of all materials and surfaces in the room [14]:

$$A = \sum_i \alpha_i \cdot S_i. \tag{2.4}$$

The influence of air absorption was originally forgotten when Sabine constructed the formula but was later added. Absorption of the air can be significant for higher frequencies in larger volumes [14]. The term for air absorption is $4mV$ and is added to Equation 2.3 giving the final expression

$$T = \frac{55.3}{c_0} \frac{V}{A + 4mV} \tag{2.5}$$

where $m$ is the power attenuation coefficient which is dependent on the temperature, humidity, and frequency [15].

Sabine's formula relies on several assumptions that can be challenging to meet in practice. If one applies Sabine's formula to a room with all surfaces at $\alpha = 1.0$, the reverberation time should be zero, but Sabine's still gives a finite reverberation time [15]. The formula also assumes that the room is sufficiently large and that the sound field within it is perfectly diffuse, meaning sound energy is evenly distributed throughout the space [11]. However, in real-world environments, this is often not the case because the room's shape, size, and placement of absorbing materials can lead to uneven sound distribution.

The formula also assumes that surfaces are either fully absorptive or reflective, yet most surfaces exhibit a combination of absorption and reflection and the texture and placement of materials can influence sound absorption in ways that the formula does not account for [11]. Accurately applying Sabine's formula depends on knowing the absorption coefficients of all surfaces in the room, which can be difficult to determine precisely. Environmental factors such as temperature and humidity also play a role, as they can alter the absorption properties of materials, leading to variations in the equivalent absorption area, and are not taken into account in Sabine's formula except for $c_0$ [26].

Other formulas have been developed to take into account that absorption and reverberation time are not a continuous progress but instead a stepwise reduction of the wave energy hitting the surface [11], but still, Sabine's is the formula used in the majority of the standards when it comes to reverberation time and absorption coefficient [8, 2, 27].

## 2.3 Methods for Measuring Sound Absorption Coefficients

There are two existing methods for measuring the absorption coefficient: the reverberation room method, as per ISO 354 [8], and the impedance tube method, detailed in ISO 10534-1 [6] and ISO 10534-2 [7].

### 2.3.1 Reverberation Room Method

The standard ISO 354 [8] describes how the reverberation room method involves measuring the reverberation time $T$ in a diffuse sound field before and after placing the test subject in the room. The standard uses Sabine's formula to calculate the reverberation time:

$$T = \frac{55.3}{c_0} \cdot \frac{V}{A} = \frac{55.3}{c_0} \cdot \frac{V}{A_S + 4mV} \tag{2.6}$$

where $V$ is the room volume ($m^3$), $c_0$ is the speed of sound in air (m/s), $A$ the equivalent absorption area ($m^2$), $A_S$ the absorption area of surfaces and objects ($m^2$), and $m$ the power attenuation coefficient. The equivalent absorption area of the test specimen $A_T$ is therefor:

$$A_T = A_2 - A_1 = 55.3 \cdot V \left( \frac{1}{c_2 T_2} - \frac{1}{c_1 T_1} \right) - 4V(m_2 - m_1). \tag{2.7}$$

The ISO 354 calculates the sound absorption coefficient $\alpha_s$ by:

$$\alpha_s = \frac{A_T}{S} \tag{2.8}$$

where $S$ is the surface area of the specimen ($m^2$).

### 2.3.2 Standing Wave Tube Method

ISO 10534-1 [6] describes a method using a straight, rigid impedance tube. In this method, a loudspeaker generates a plane sinusoidal sound wave inside the tube, and a probe microphone is employed to measure the resulting sound field. The interaction between the incident sound wave ($p_i$) and the reflected wave ($p_r$) within the tube creates a standing wave pattern. By analyzing this pattern, the sound absorption coefficient $\alpha$ can be calculated.

The sound absorption coefficient is determined using the following equation:

$$\alpha = \frac{4 \times 10^{\Delta L/20}}{(10^{\Delta L/20} + 1)^2} \tag{2.9}$$

where $\Delta L$ is the difference in sound pressure levels at maximum and minimum pressure points.

### 2.3.3 Normal-Incidence Impedance Tube Method

ISO 10534-2 [7] explains a method where plane waves are generated in the impedance tube with the test sample mounted at one end, and the sound pressure is measured at two fixed locations near the sample. The standard explains how the acoustic transfer function is calculated to determine the normal-incidence sound absorption coefficient $\alpha_n$ and surface impedance:

$$\alpha_n = 1 - |r|^2 = 1 - r_r^2 - r_i^2. \tag{2.10}$$

The reflection coeffienct $r$ is calculated from:

$$r = e^{i \cdot 2 \cdot k_0 \cdot L_a} \cdot \left( \frac{H_{12} - e^{-i \cdot k_0 \cdot x_1}}{e^{i \cdot k_0 \cdot x_1} - H_{12}} \right) \tag{2.11}$$

where $x_1$ is the distance between the test sample surface and the furthest microphone, $L_a$ is the distance between the microphones, $k_0$ is the complex wave number, and $H_{12}$ is the transfer function from microphone position one to two [7, 28].

### 2.3.4 Uncertainties and limitations in the methods

Each of the measurement methods has its own limitations and uncertainties that affect their accuracy and applicability in different contexts.

None of the existing methods is developed or adapted to be used in situ inside or outside buildings [11] and can therefore not be used during verification and precisely pinpointing areas where the absorption coefficient is inadequate in buildings.

The frequency range is a limitation for all three methods. ISO 354 [8] states that measurement results below 100 Hz can be difficult because of the reverberation room's low modal density. ISO 10534-1 and ISO 10534-2's frequency range depend on the tube's length and diameter and the placements of the microphones, making it difficult to construct tubes to measure low frequencies [6, 7].

Another major limitation of ISO 10534-1 and ISO 10534-2 is that they only measure in normal incident, not in diffuse field [6, 7], which makes them more effective for laboratory-based measurements of small samples.

ISO 354 has an uncertain when it comes to reproducibility [8]. Studies have shown that laboratories get different results when measuring the same sample [3]. This can be due to the shape of the room and how and if a diffuse field is reached. The

size and thickness of the absorber can also affect the results [2], and the mounting conditions also affect the results [1]. The edge effect is one of the consequences when measuring absorbers. The edge effect can lead to overestimation or underestimation of absorption performance, creating further uncertainties in the measurement data [3, 8]. It's recommended that the sample should be as large as possible to avoid this [8], but ISO 354 doesn't measure ceiling tiles in the same mounting conditions as in the world [2]. This lack of standardization of mounting conditions for ceiling absorbers with large cavities can affect the results by leaving the edges exposed or having a support structure in the room [1, 29].

## 2.4 Transfer matrix model

The transfer matrix model is a model developed by Vigran and used to analyze the propagation of sound waves through layered media, such as sound absorbers [11]. Vigran [11] explains that in the model, the relationship between the acoustic pressure $p$ and particle velocity $v$ at two points within the medium is expressed using a transfer matrix. This matrix accounts for the interactions of the wave with each layer and allows us to calculate important acoustic properties such as impedance and absorption.

The general form of the transfer matrix equation is:

$$\begin{bmatrix} p_{n-1} \\ v_{n-1} \end{bmatrix} = \begin{bmatrix} a_{11} & a_{12} \\ a_{21} & a_{22} \end{bmatrix} \begin{bmatrix} p_n \\ v_n \end{bmatrix} \tag{2.12}$$

Here, $p_n$ and $v_n$ represent the pressure and particle velocity at the $n$-th layer, while $p_{n-1}$ and $v_{n-1}$ correspond to the previous layer. The elements of the matrix $a_{11}, a_{12}, a_{21}$, and $a_{22}$ describe how the wave is modified as it travels through the layer.

The input impedance $Z_g$ at the beginning of the absorber and the load impedance $Z_L$ at the end are related by the transfer matrix:

$$Z_g = \frac{p_{n-1}}{v_{n-1}} = \frac{A_{11}Z_L + A_{12}}{A_{21}Z_L + A_{22}}. \tag{2.13}$$

Using the input impedance, we can calculate the absorption coefficient $\alpha$, which quantifies the fraction of incident acoustic energy absorbed by the material:

$$\alpha = 1 - |R_p|^2 \tag{2.14}$$

where $R_p$ is the pressure reflection coefficient, accounting for the angle of incidence in a diffuse field.

The reflection coefficient is given by:

$$R_p = \frac{Z_g \cos\varphi - \rho_0 c_0}{Z_g \cos\varphi + \rho_0 c_0} \tag{2.15}$$

where, $\rho_0$ is the density of air, $c_0$ is the speed of sound in air, and $\varphi$ is the angle of incidence.

The wave propagation in the medium can be described by the superposition of forward and backward traveling waves:

$$p(x) = A \cdot \mathrm{e}^{-jkx} + B \cdot \mathrm{e}^{jkx} \tag{2.16}$$

$$v(x) = \frac{1}{Z_c}\left(A \cdot \mathrm{e}^{-jkx} - B \cdot \mathrm{e}^{jkx}\right) \tag{2.17}$$

where $Z_c$ is the characteristic impedance of the medium, and $k$ is the wave number.

When considering a specific layer of the material, the relationship between pressure and velocity at the two boundaries of the layer can be expressed using a more detailed transfer matrix:

$$\begin{bmatrix} p_1 \\ v_1 \end{bmatrix} = \begin{bmatrix} \cos(kd) & jZ_c \sin(kd) \\ \frac{j\sin(kd)}{Z_c} & \cos(kd) \end{bmatrix} \begin{bmatrix} p_2 \\ v_2 \end{bmatrix} \tag{2.18}$$

where $d$ is the thickness of the layer.

For more complex cases, such as when the angle of incidence is not normal, it is useful to express the wave number as a propagation coefficient $\Gamma = jk$. The general form of the transfer matrix for an inconsistent angle of incidence $\varphi$ is:

$$\begin{bmatrix} p_1 \\ v_1 \end{bmatrix} = \begin{bmatrix} \cosh(\Gamma d \cdot \cos\varphi) & \frac{Z_c \sinh(\Gamma d \cdot \cos\varphi)}{\cos\varphi} \\ \frac{\sinh(\Gamma d \cdot \cos\varphi)}{Z_c \cdot \cos\varphi} & \cosh(\Gamma d \cdot \cos\varphi) \end{bmatrix} \begin{bmatrix} p_2 \\ v_2 \end{bmatrix}. \tag{2.19}$$

This more general form takes into account the effect of oblique incidence on wave propagation through the material, providing a comprehensive understanding of how the sound absorber behaves under different conditions.

The statistical absorption factor $\alpha_{stat}$ represents the mean absorption over all angles of incidence, which is crucial for practical applications where sound arrives from various directions. It is defined as:

$$\alpha_{stat} = 2\int_0^{\pi/2} \alpha(\varphi)\sin(\varphi)\cos(\varphi)\,\mathrm{d}\varphi = 2\int_0^{\pi/2} \left[1 - |R_p|^2\right]\sin(\varphi)\cos(\varphi)\,\mathrm{d}\varphi \tag{2.20}$$

where, $\varphi$ is the angle of incidence, and $\alpha(\varphi)$ is the absorption coefficient at that angle. The reflection coefficient $R_p$ is given by:

$$R_p = \frac{Z_g \cos\varphi - Z_0}{Z_g \cos\varphi + Z_0} = \frac{Z_n \cos\varphi - 1}{Z_n \cos\varphi + 1} \tag{2.21}$$

where $Z_0 = \rho_0 c_0$ is the characteristic impedance of the medium, and $Z_n = \frac{Z_g}{Z_0}$ is the normalized impedance. This form highlights how the impedance mismatch and the incidence angle affect sound's reflection and absorption.

Vigran's transfer matrix model is possible to build out depending on how many layers and what type of material there is. The previous equation shows a 2x2-matrix, but for porous elastic materials, a 6x6-matrix is needed. The transfer matrix model can be altered for many different layers and materials and can also be used for calculating transmission and reduction index for multilayered elements [11].

BILD

### 2.4.1 Acoustic Impedance models

The acoustic impedance, $Z$, in Vigran's model can be specified in different ways. The most common one to follow is the model developed by Delany and Bazley in 1970 [11]. It is widely used due to its simplicity and effectiveness in predicting acoustic behavior in porous materials. It uses a set of regression equations derived from empirical measurements on highly porous materials, such as mineral wool, with near-perfect porosity [30]. The model was then developed by fitting the data, with the flow resistivity and the frequency as parameters [11]. The final results of the work produced two equations that can be implemented in the transfer matrix model. The characteristic impedance $Z_c$ and $\Gamma$ from Daleny and Bazley are the following:

$$Z_c = \rho_0 c_0 \left[1 + 0.0571 \cdot E^{-0.754} - j \cdot 0.087 \cdot E^{-0.732}\right] \tag{2.22}$$

$$\Gamma = j\frac{\omega}{c_0} \left[1 + 0.0978 \cdot E^{-0.700} - j \cdot 0.189 \cdot E^{-0.595}\right] \tag{2.23}$$

where $\omega = 2\pi f$ and $E$ is the quantity expressed $E = \frac{\rho_0 f}{\sigma}$, and $\sigma$ is the flow resistivity [11]. Delany and Bazley's model is valid in a frequency range where

$$10 \leq \frac{f}{\sigma} \leq 1. \tag{2.24}$$

From Daleny and Bazley's measurement data, Miki creates a new regression method [31]. Miki's model makes sure that the impedance function satisfies the

positive-real property and is reliable in a larger frequency range than Daleny and Bazley's [32]. The characteristic impedance $Z_c$ and $\Gamma$ from Miki are the following:

$$Z_c = \rho_0 c_0 \left[1 + 0.070 \left(\frac{f}{\sigma}\right)^{-0.632} - j0.107 \left(\frac{f}{\sigma}\right)^{-0.632}\right] \tag{2.25}$$

$$\Gamma = \frac{\omega}{c_0} \left[0.160 \left(\frac{f}{\sigma}\right)^{-0.618} - j \left(1 + 0.109 \left(\frac{f}{\sigma}\right)^{-0.618}\right)\right] \tag{2.26}$$

Another commonly used model for $Z_c$ and $\Gamma$ is by Mechel. Mechels model uses a theoretically based procedure for low frequency and a curve-fitting procedure on measured data at high frequencies [11]. For lower frequencies, Mechel has porosity as a parameter, together with flow resistivity and frequency, but for mid and high frequencies, only flow resistivity and frequency [33]. The model uses $E$ as a transition value between the lower frequency equation and the higher frequency equation.

Figure 2.3, 2.4 and 2.5 shows a comparison between the three models.

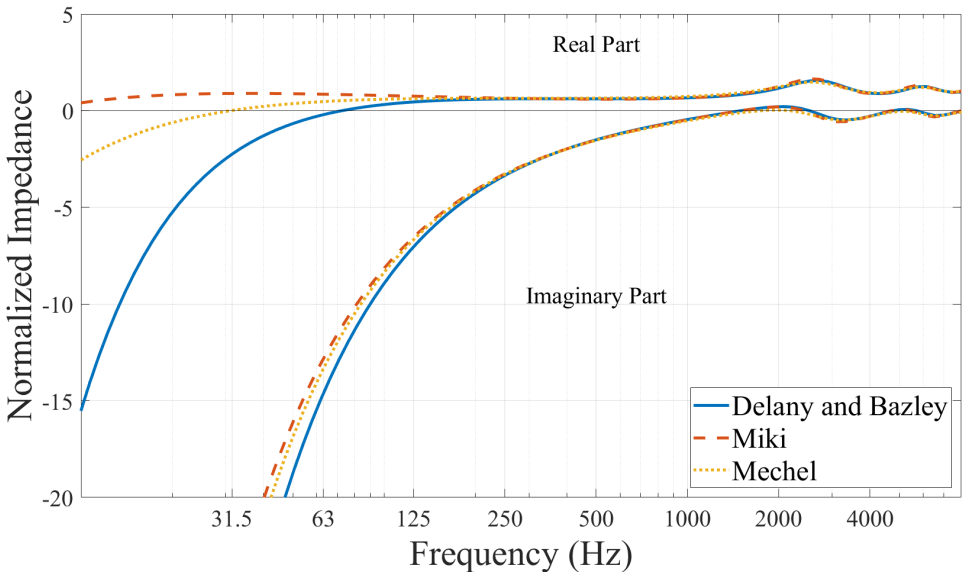


**Figure 2.3:** Real and imaginary part for the input impedance (normal incident) for an absorber with a thickness of 50 mm, airflow resistivity $\sigma = 10\ 000\ \text{Pa} \cdot \text{s/m}^2$, directly on a hard backing.

Figure 2.3 represents the real and imaginary part of the input impedance $Z_c$ for the different models, calculated for normal incident. Here, it's visible that Delany-Bazley's model becomes reliable above approximately 70 Hz, as the real part of the impedance is negative below this frequency, indicating non-physical behavior. Miki's model exhibits a positive real part across all lower frequencies, while Mechel maintains a positive real part above 31.5 Hz.

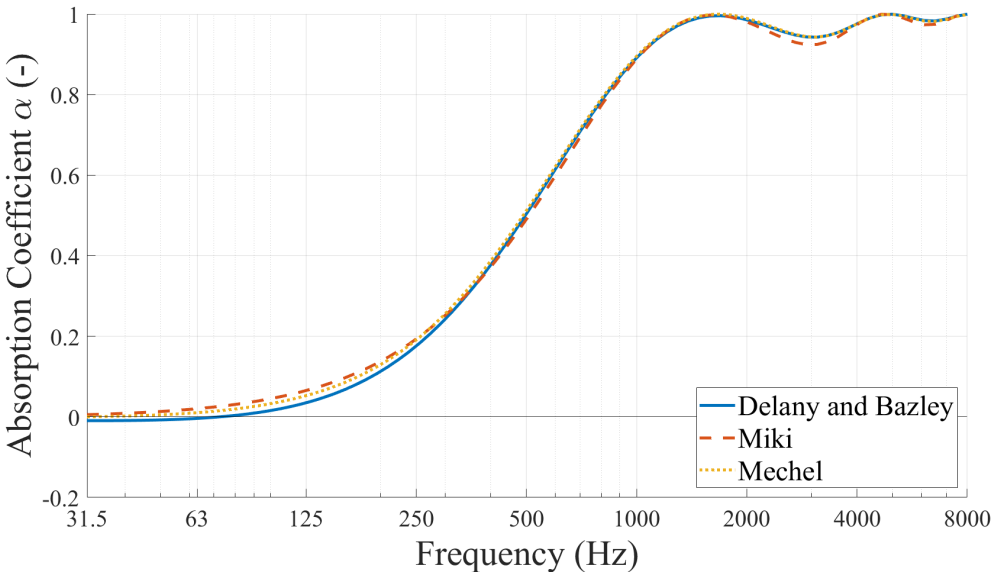


**Figure 2.4:** Comparison between Delany-Bazley, Miki and Mechel's models for a 50 mm absorber, airflow resistivity $\sigma = 10\ 000\ \mathrm{Pa \cdot s/m^2}$ mounted directly on hard back.

Figure 2.4 and 2.5 illustrate a comparison between the three different models for two different cases. Figure 2.4 shows that Delany-Bazley's model is not reliable below approximately 70 Hz because the absorption coefficient becomes negative, which is not physically possible. From around 250 Hz, the results for the different models have very little.

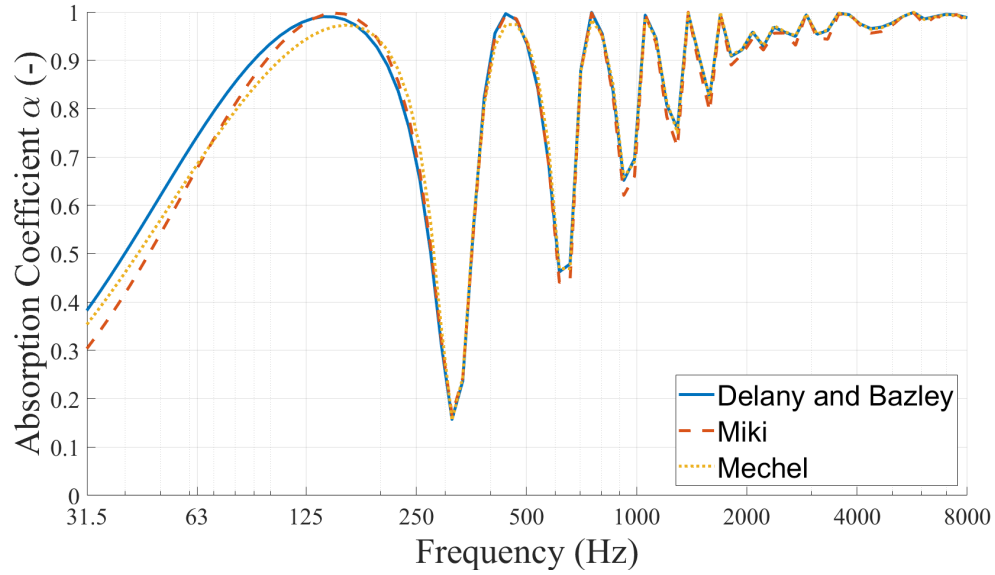


**Figure 2.5:** Comparison between Delany-Bazley, Miki and Mechel's models for a 50 mm absorber, airflow resistivity $\sigma = 10\ 000\ \mathrm{Pa \cdot s/m^2}$ mounted with an airgap of 500 mm

Figure 2.5 does not have any negative absorption coefficient and shows the same

pattern as Figure 2.4 where the results are very similar from 250 Hz. In the case of a larger air gap, the results below 250 Hz vary more between the different models.

### 2.4.2 Calculating the Edge Effect

The transfer matrix model calculates for infinite large samples, which is never the case in real life. In measurement in the reverberation room, the edge effect appears because diffraction happens along the edges, making the absorption area larger than the geometrical area [11]. Thomasson [34] developed a formula for calculating $\alpha_{stat}$ with regard to the edge effect:

$$\alpha_{stat} = \frac{4\mathrm{Re}Z_n}{\pi} \int_0^{\pi/2} \int_0^{2\pi} \frac{\sin\varphi}{|Z_n + Z_f|^2} d\varphi d\theta. \tag{2.27}$$

Here $Z_f$ is the field impedance, a function of the shape, dimension, velocity distribution, frequency, and angel incident. The direction of the incident is specified by both the angel $\varphi$ and azimuth angel $\theta$.

# 3

# Methodology

*This chapter outlines the selected model, simulation techniques, and validation methods used to ensure the study's reliability and accuracy. Following the Model and Simulation cycle, the elements of the processes of problem definition, conceptual and computational modeling, and model verification and validation are presented. The real-life validation follows the ISO 354 [8], ISO 3382-2 [27], and ISO 10534-2 [7] standards and the equipment and procedures used in the study are explained.*

## 3.1 Modeling and Simulation

Simulations are a type of experiment, but the subject studied is not a perfect reflection of reality [35]. Therefore, it's important to design the model to best represent reality. This can be done by incorporating design, verification, and validation [36]. This study followed the model and simulation cycle presented by Säfsten [36], which can be broken down into seven steps:

1. **Understand the problem:** Define the scope and objectives in the real world.
2. **Simplify and structure:** Choose relevant aspects and connections and build a conceptual model representing the system.
3. **Mathematics:** Convert the conceptual model into a numerical form.
4. **Process the mathematics:** Validation of the model, making sure it reflects the requirements.
5. **Interpret:** Convert the mathematical results back into the context of the real situation.
6. **Validate:** Ensure the model reflects real-world phenomena by collecting data.
7. **Present:** Communicate the results and conclusions.

## 3.2 Problem definition and Conceptual Modeling

The initial phase of this study focused on defining the problem through an extensive literature review. This included a detailed examination of the system's key objectives, limitations, and broader context. Particular attention was given to understanding the function and construction of absorbers and the behavior of sound waves in enclosed spaces.

Once the problem was defined, the next step was to simplify and structure the problem. The literature review led to the discovery and understanding of Vigran's transfer matrix model [11]. The transfer matrix model suited different layers and their response and interaction with sound waves. The critical variables within the model were easy to identify, and the conceptual model laid the ground for the computational model.

## 3.3 Mathematics and the computational model

This step translated the conceptual model into a computation model using programming and numeric software. The model for this study needed to be flexible, allowing adjustments to be made and integrating real-life data and parameters to reflect reality.

The calculations and simulations were done in MATLAB, a programming and numeric computer platform. MATLAB can be used to analyze data, develop algorithms, and create models with a programming language that expresses matrix and array mathematics directly [37].

The model was built based on Vigran's transfer-matrix model and used Delany and Bazley's wave propagation theory. It started with simulating a porous absorber on hard backing before evolving it to a more complex model with an air gap between the absorber and the hardback. The model calculated in 1/3-octave bands.

The model verification was done continuously throughout the development to ensure the computational model correctly followed the conceptual model. The verification involves comparing the model's outputs against known solutions or benchmarks, product data or data given in books, ensuring the algorithms and calculations perform correctly, which could be.

## 3.4 Validation of the model

Model validation is essential to ensure the model accurately represents real-world phenomena. In this phase, empirical data was collected from the field to compare with the model's outputs. The validation identifies potential errors between the model and real-world data. This leads to necessary model improvements and limitations for all models and methods. For this study, two validations were conducted: one using a commercial software based on the Transfer Matrix Model

and the other validation through real-life measurements.

### 3.4.1 Software validation - Norflag

Norflag, also known as Winflag, was created by Tor Erik Vigran and is a software used to predict the acoustic performance of constructions combining different material layers [38]. The program can calculate the absorption coefficient, the impedance, and the sound reduction index based on the same transfer matrix model mentioned in 2.4 [39]. Winflag allows you to customize the material data in terms of thickness and flow resistivity.

The program offers two options for absorption coefficient: diffuse field or reverberation room.

The diffuse field calculates a mean value for all angles of incidence and produces a $\alpha_{stat}$ with the same equation as Equation 2.20 [39].

In the reverberation room options, the absorption coefficient is also integrated over the angle of incidence, but the limited size of the absorbent is taken into account [39]. The diffraction effects of the edges, leading to the absorption coefficient in some cases being larger than 1.0, are also considered. Using Equation 2.27 formed by Thomasson [34], the edge effect is considered when using the reverberation room option in Norflag.

To validate the model, several standard situations were created in Norflag and compared to the model, both using the diffuse field option and the reverberation room option. The situation for the measurement validation was also created and compared.

### 3.4.2 Measurment validiation

The sound absorption coefficient was calculated according to ISO 354 [8], and the measurement followed ISO 3382 [27] since the study didn't have access to a reverberation room. The measurement was done in an office using the existing absorbent ceiling tiles. Two measurements were taken, one with the ceiling mounted and one with no ceiling. Since the tiles had no identifying tags, additional characteristics, including airflow resistivity, could not be determined from product information. The impedance tube method [7] was then used to determine further characteristics of the absorbent. The impedance tube available for this study does not have space to measure the absorbent with a large air gap. Still, airflow resistivity is a material aspect, where the absorption coefficient depends on the construction. Therefore, the impedance tube method could still be used to determine the airflow resistivity of the tiles.

#### 3.4.2.1 Room Measurement

The room used for this measurement is shown in Figure 3.1 and is a small office. Two walls of the room were covered in gypsum, and two sides with windows. The

floor had a thinner carpet, and the ceiling had absorbing ceiling tiles. When the ceiling tiles were removed, the roof would be concrete and have various ventilation canals and installations.

**Figure 3.1:** The room used during the measurement.

The length and width of the room were 4 m, respectively, 2.3 m, and can be seen in Figure 3.2. The height of the room with the ceiling was 2.38 m. Without the ceiling tiles, the height reached a maximum of 2.95 m but was also interrupted by ventilation canals and other installations, as seen in Figure 3.1.

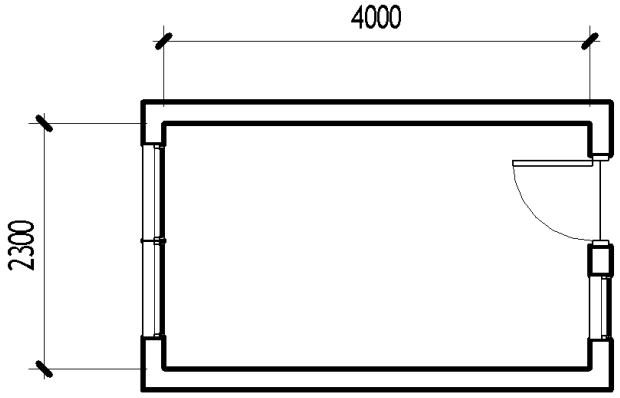


**Figure 3.2:** View of the dimensions and elements of the room.

During the room measurement, the following equipment was used:

- Nor275 hemi-dodecahedron loudspeaker
- Power Amplifier Nor280

- Nor140 Sound analyser
- Omnidirectional microphones Nor1209 1/2" microphone preamplifier
- Sound Calibrator Nor1255
- Stand for the analyzer
- Balloons
- Pen or needle
- Some objects to add to the room to avoid flatter echo and achieve a diffuse field.
- Hearing protection

The measurement followed the integrated impulse response method in ISO 3382-2, where popping a balloon was used as the impulse response source [27]. The measurement was done with two different source positions and six microphone positions for each source position, giving 12 source-microphone combinations according to the precision method [27].

Calculations of reverberation time were done with the Nor140 Sound analyser, and the reverberation time, $T_{20}$, with a 20 dB decay was calculated according to ISO 3382-2 and extracted from the analyser in 1/3-octave bands [27, 40].

The values could then be calculated according to ISO 354 and Equation 2.7 and 2.8. Since the volume of the room was small, the air absorption could be neglected, and the room temperature could be assumed to be the same throughout the whole measurement. The formula for the equivalent absorption area of the test specimen $A_T$ was simplified to

$$A_T = A_2 - A_1 = \frac{55.3}{c}\left(\frac{V_2}{T_2} - \frac{V_1}{T_1}\right). \tag{3.1}$$

Given the variation in room volume, $A_T$ was calculated under two scenarios: one with the two different room volumes and another where both volumes were set to the larger value. This approach was necessary due to limited guidance on addressing significant volume changes.

The calculations for $A_T$ and the absorption coefficient, Equation 2.8 were done in MATLAB by taking the arithmetic mean of the individual reverberation times for each frequency for $T_1$ and $T_2$ respectively [8] and calculating the absorption coefficient by using Sabine's formula $A = \alpha \cdot S$. The results for the absorption coefficient were used to validate and compare with the model.

#### 3.4.2.2 Measurement of the Ceiling Tile

The airflow resistivity was measured using the standardized transfer-function method by ISO 10534-2 [7], using an impedance tube. The test sample was cut from a ceiling tile used in the room measurements in the previous section, Section 3.4.2). The tile was made of glass fiber, and Figure 3.3 shows a cross-section of the tile.

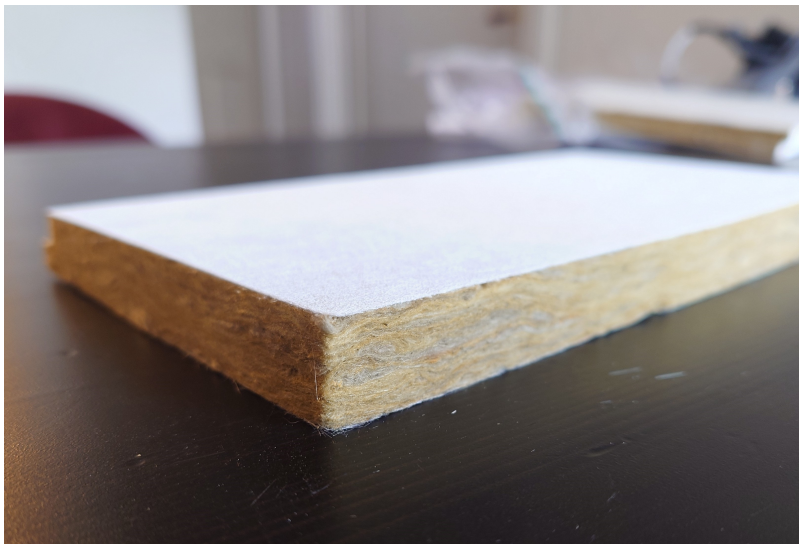

**Figure 3.3:** Cross-section of the ceiling tile used in the measurements.

As shown in Figure 3.3, the tile features a thin surface layer of glass fiber, which gives it a white appearance. The tile has a square geometry with dimensions of 600 mm per side and a thickness of 18 mm. The test sample was cut using a precision instrument to match the exact shape and size of the impedance tube to ensure that the absorber was placed in the tube with a perfect fit, ensuring no air gap and close contact with the tube walls.

During the tube measurement, the following equipment was used:

- Loudspeaker
- Power Amplifier
- SQuadriga III analyser
- Microphone
- A tube construction

Figure 3.4 shows the setup for the measurement and the construction of the tube.

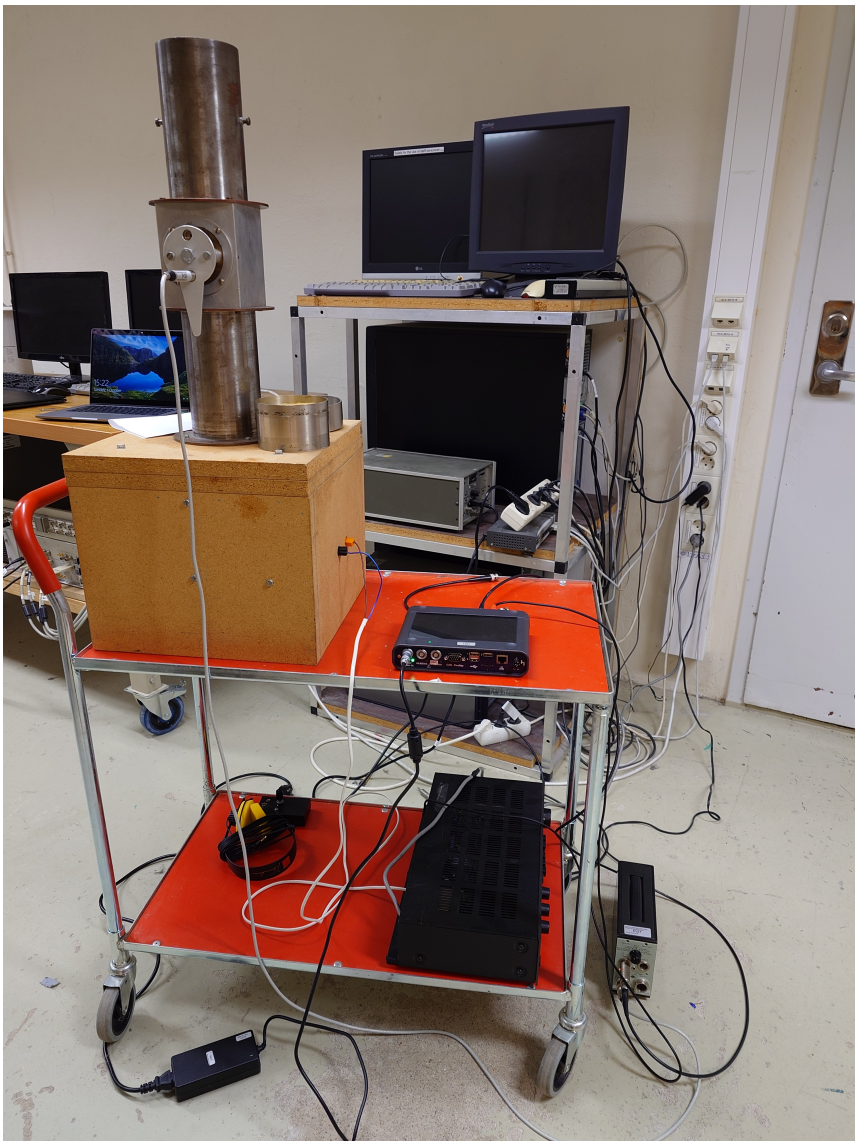

**Figure 3.4:** The setup and equipment used for the tube measurement.

The SQuadriga analyzer was used to generate pink noise and process the data. A loudspeaker was placed at one end of a 0.1 m diameter impedance tube, with the test sample mounted at the opposite end. The microphone had two fixed positions, 0.265 m and 0.215 m from the sample, and the microphone position was changed using a switch.

The lower and upper frequency limits, $f_l$ and $f_u$, were calculated based on ISO 10534-2:

$$f_u < \frac{0.45 \cdot c_0}{D} \tag{3.2}$$

$$s > 0.015 \cdot \frac{c_0}{f_l} \tag{3.3}$$

with $D$ as the tube diameter and $s$ as the microphone spacing. The lower

frequency limit occurs at 100 Hz, an $f_l$ was set to 200 Hz, and the upper frequency limit to $f_u = 2000$ Hz.

Four samples were measured for 30 seconds at each microphone position, with each test repeated three times. The SQuadriga provided transfer functions $H_{12}$, which were converted to Mat-files in Artemis [41] and analyzed using MATLAB.

The reflection coefficient $R$ was calculated from the transfer function $H_{12}$ according to ISO 10534-2:

$$R = e^{i \cdot 2 \cdot k_0 \cdot L_a} \cdot \left( \frac{H_{12} - e^{-i \cdot k_0 \cdot a_s}}{e^{i \cdot k_0 \cdot a_s} - H_{12}} \right) \tag{3.4}$$

Impedance was derived as $Z = \frac{1+R}{1-R}$ and and the absorption coefficient $\alpha$ was computed as $\alpha = 1 - |R|^2$.

Airflow resistivity was then estimated by fitting $\alpha$ to a theoretical model using grid search and minimizing the root mean square deviation (RMSD) [28]. The best-fit value was approximately 104 000 $\mathrm{N \cdot s/m^3}$.

# 4

# Results

*This chapter presents the model's results. The first section presents the simulation's validation with the measurement and Norflag results, followed by the simulation results for different scenarios.*

## 4.1 Validation

This section presents the results from the validation of the model using both measurement data and simulations. The goal is to compare the simulated absorption coefficients with those obtained from room measurements and for calculations in Norflag.

Figure 4.1 displays the absorption coefficient calculated from the room measurement. Given the variation in room volume, the absorption coefficient was calculated under two scenarios: one with the two different room volumes and another where both volumes were set to the larger value. Details on the measurement process and the calculation methods can be found in Section 3.4.2.

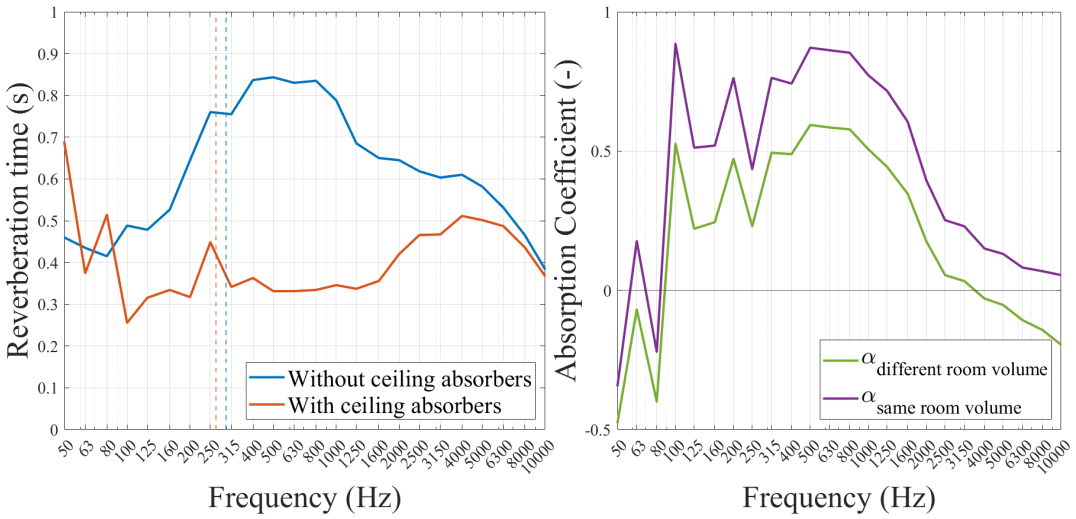


**(a)** Measured reverberation time of the room.

**(b)** Calculated absorption coefficient of the room.

**Figure 4.1:** Results from the measurement showing the reverberation time and calculated absorption coefficient. The dotted line in (a) shows the Schroeder frequency for each room volume.

In Figure 4.1 (b) one can see that the absorption coefficient curves shift depending on which volumes are accounted for. The results from Figure 4.1 reveal a decay in the absorption coefficient above 800 Hz. This decay may be caused by the surface layer on the tiles, which could limit sound absorption at higher frequencies, or it could be a result of standing waves in the room, suggesting the absence of a diffuse field. The room's Schroeder frequency, $f_{Schroeder}$ is shown in Figure 4.1 with a dotted line and is approximately 300 Hz without ceiling absorbers and approximately 260 Hz with ceiling absorbers. The Schroeder frequency indicates that the sound field can not be assumed to be diffuse below this threshold, making the results uncertain.

Figure 4.2 presents the results from the tube measurement and the fitted model for airflow resistivity determined by grid search.

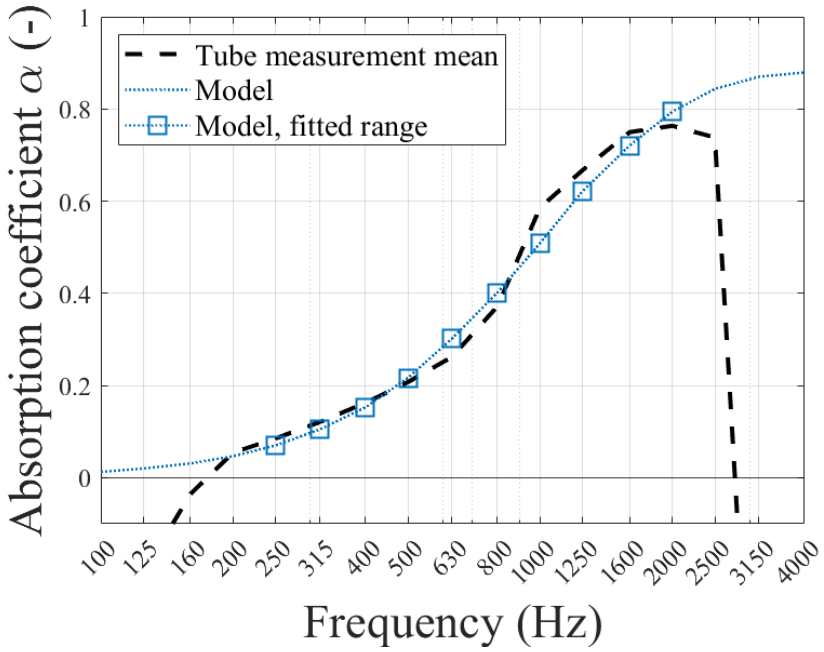


**Figure 4.2:** Absorption coefficient over frequencies from the tube measurement and the fitted curve from modeled with airflow resistivity $\sigma$=104 000 Pa $\cdot$ s/m$^2$.

The curve in Figure 4.2 shows that the modeled data with an airflow resistivity of $\sigma$ = 104 000 Pa $\cdot$ s/m$^2$ closely aligns with the measured values from the tube experiment. It's important to note that these results for the absorption coefficient in this case are not directly comparable since the interest of this study is air cavities which the tube measurement used in this study did not allow.

Figure 4.3 demonstrates the results from Norflag, calculated using Delany-Bazley's impedance model in a diffuse field, with the same airflow resistivity and thickness of the absorber as the room measurement.

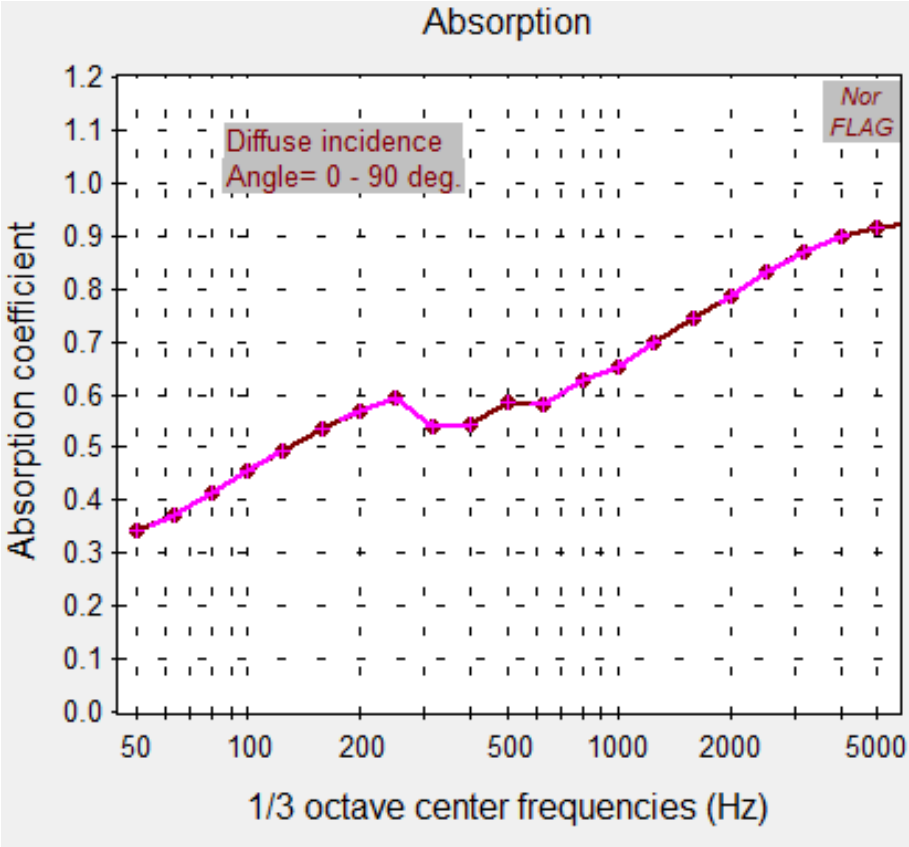


**Figure 4.3:** Results from Norflag calculated with Delany-Bazley's model in diffuse field for airflow resistivity $\sigma$=104 000 Pa $\cdot$ s/m$^2$ and thickness of the absorber 18 mm.

The curve in Figure 4.3 follows the expected path, where the absorption gets higher for higher frequencies. The curve also has a bump around 200 Hz, indicating some sort of quarter-wavelength behavior.

Figure 4.4 shows the results from the simulation for the same condition as the room measurement: $\sigma$=104 000 Pa $\cdot$ s/m$^2$, tiles thickness equal to 18 mm and an air gap of 552 mm.

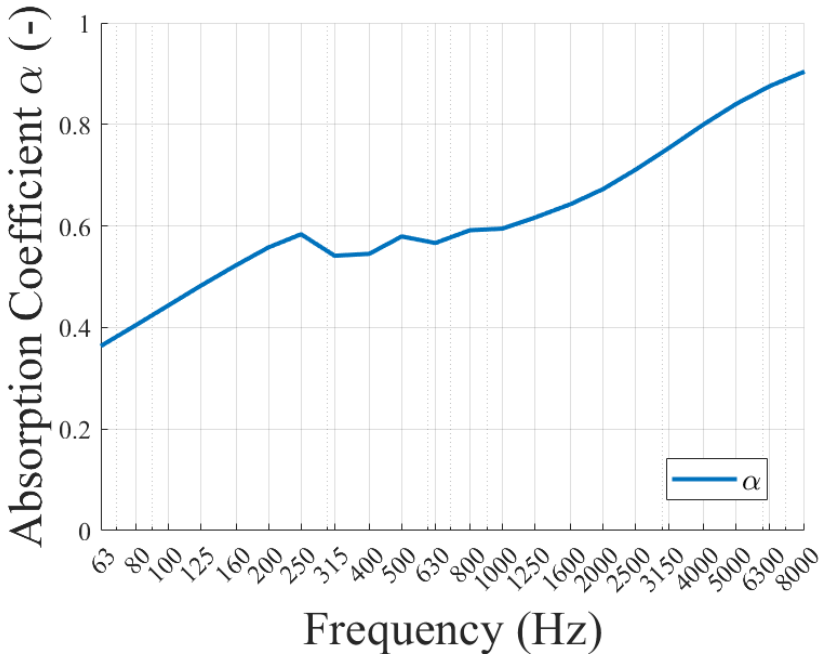


**Figure 4.4:** Absorption coefficient over frequencies for the developed model, with the same properties as the room measurement. Airflow resistvity set to $\sigma$=104 000 Pa $\cdot$ s/m$^2$, thickness of the absorber 18 mm and air gap 552 mm.

The curve in Figure 4.4 shows a similar pattern as the Norflag calculation, where the absorption increases with the frequencies and an elevation of around 200 Hz, but the absorption coefficient doesn't go as high as the results from the Norflag calculations.

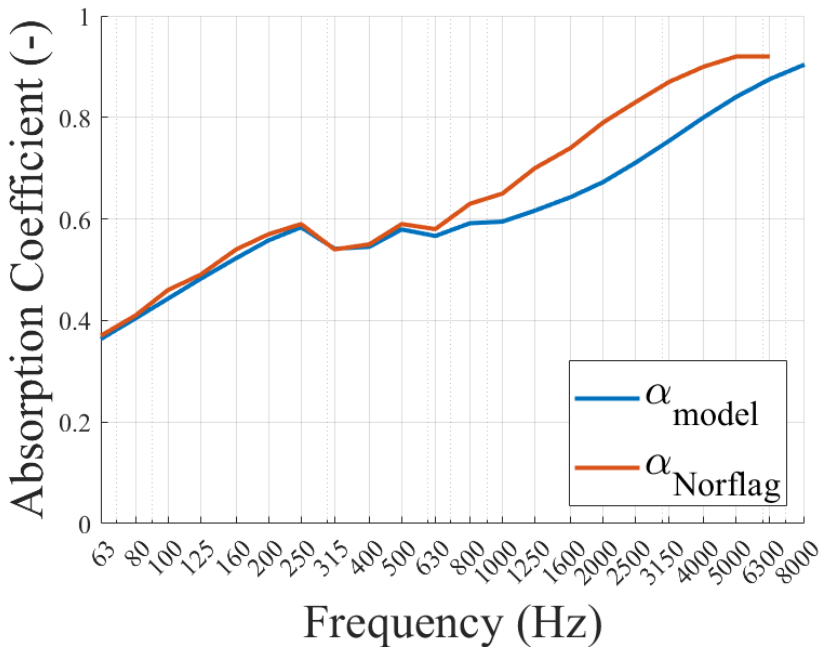


**Figure 4.5:** Comparison of absorption coefficient across frequency for the developed model and Norflag simulation.

The comparison in Figure 4.5 indicates that the developed model closely follows the Norflag simulation up to around 800 Hz. However, compared with the room measurement data in Figure 4.1, the results diverge for all frequencies.

## 4.2 Simulations

This section displays the results from the simulations in 1/3-octave bands. Two different thicknesses of the absorber was chosen together with four diffrent air gap (0 mm, 500 mm, 1000 mm, 1500 mm). These conditions were then repeated for four different airflow resistivities, $\sigma$=10 900 Pa $\cdot$ s/m$^2$, $\sigma$=39 620 Pa $\cdot$ s/m$^2$, $\sigma$=64 000 Pa $\cdot$ s/m$^2$, and $\sigma$=104 690 Pa $\cdot$ s/m$^2$. The airflow resistivity and the thickness of the absorber were chosen by looking at data for typical acoustical ceiling tiles.

Figure 4.6 shows the results from the simulation with the airflow resistivity set to 10 900 Pa $\cdot$ s/m$^2$ and the thickness of the absorber being 20 mm and 40 mm.

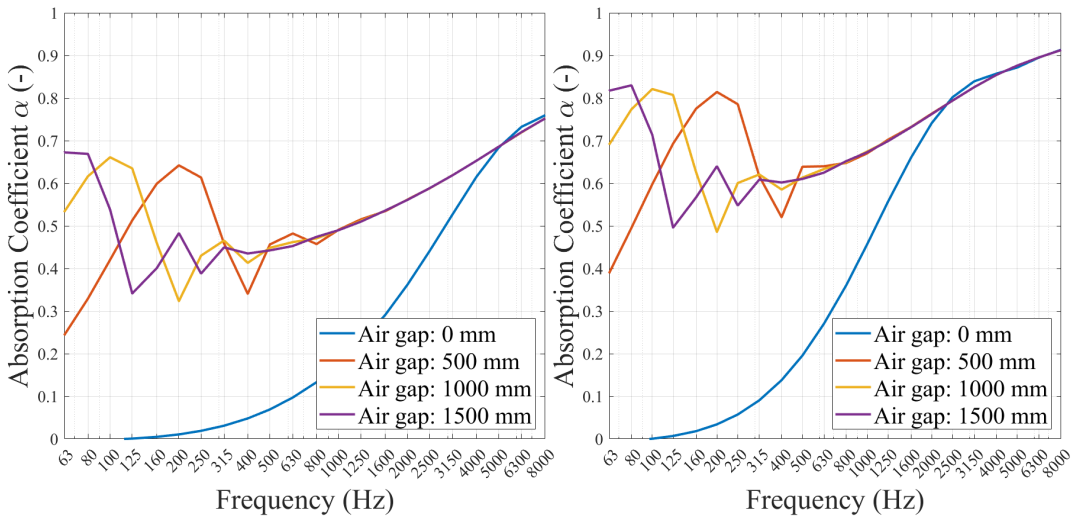


**(a)** Thickness of the absorber: 20 mm

**(b)** Thickness of the absorber: 40 mm

**Figure 4.6:** The two figures compare the absorption coefficient as a function of frequency for different air gap, and for two absorber thicknesses. The airflow resistivity is fixed at 10 900 Pa · s/m$^2$ in both cases.

Figure 4.6 shows that a thicker absorber increases the absorption coefficient for this airflow resistivity. For the absorber with no air gap, the absorption mainly increases in the mid to high frequencies. The curves for the different air gaps are shifted upwards by approximately 0.1 across all frequencies. At lower frequencies, the curves for the air gaps exhibit a peak followed by a dip before stabilizing. Above approximately 800 Hz, the absorption for different air gaps aligns and shows minimal variation.

Figure 4.7 shows the results from the simulation with the airflow resistivity set to 39 620 Pa · s/m$^2$ and the thickness of the absorber is 20 mm and 40 mm.

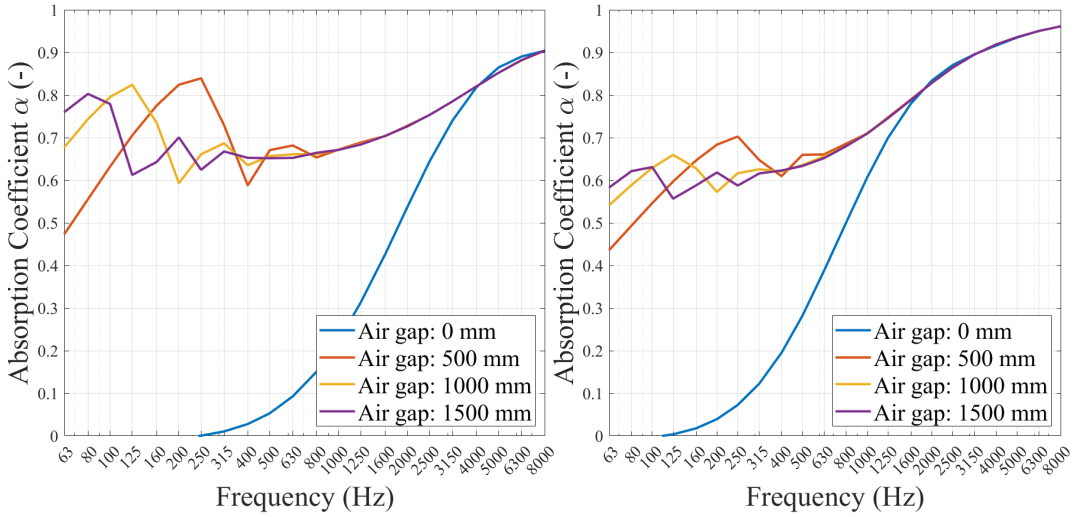


**(a)** Thickness of the absorber: 20 mm

**(b)** Thickness of the absorber: 40 mm

**Figure 4.7:** The two figures compare the absorption coefficient as a function of frequency for different air gap, and for two absorber thicknesses. The airflow resistivity is fixed at 39 260 $\mathrm{Pa} \cdot \mathrm{s/m^2}$ in both cases.

Figure 4.7 shows that the curves for the different air gaps align from 800 Hz. With the increased thickness, the absorber without an air gap shows improved absorption across all frequencies, while the curves for the air gaps (500 mm, 1000 mm, 1500 mm) only show improvements at higher frequencies. Notable is that at lower frequencies, the absorption coefficient decreases with a thicker absorber, and the peaks and dips become less distinct.

Figure 4.8 shows the results from the simulation with the airflow resistivity set to 62 930 $\mathrm{Pa} \cdot \mathrm{s/m^2}$ and the thickness of the absorber being 20 mm and 40 mm.

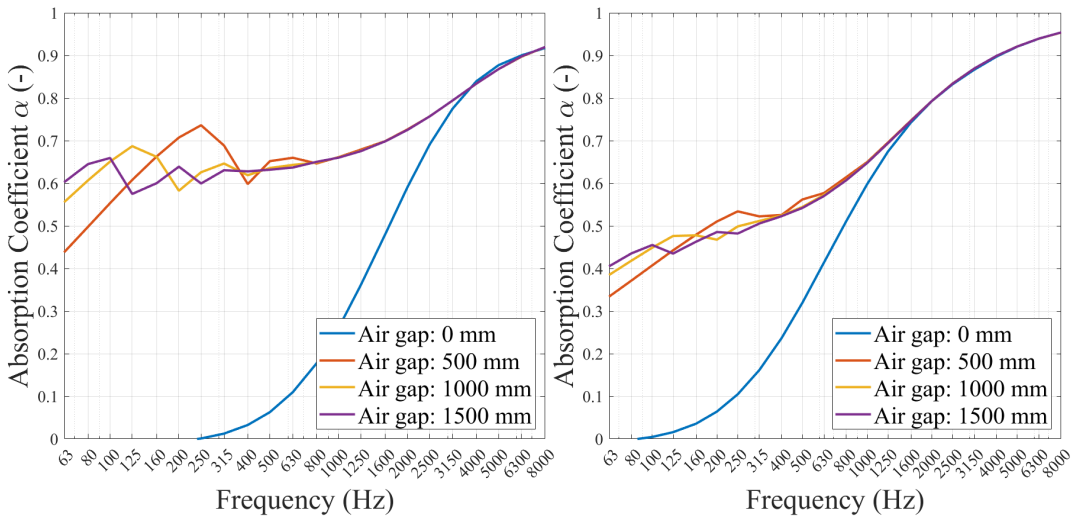


**(a)** Thickness of the absorber: 20 mm

**(b)** Thickness of the absorber: 40 mm

**Figure 4.8:** The two figures compare the absorption coefficient as a function of frequency for different air gap, and for two absorber thicknesses. The airflow resistivity is fixed at 62 930 Pa · s/m$^2$ in both cases.

Figure 4.7 shows that above 800 Hz, the curves for the different air gaps are the same. It also shows that increasing the thickness of the absorber enhances the absorption across all frequencies for the absorber without an air gap. However, for the air gaps (500 mm, 1000 mm, 1500 mm), an absorber thickness only enhances absorption at the higher frequencies. For the lower frequencies, the absorption decreases with a thicker absorber, same as in Figure 4.7. Additionally, the distinct peaks in the lower frequencies seen for the thinner absorber decrease significantly with a thicker absorber.

Figure 4.9 shows the results from the simulation with the airflow resistivity set to 104 690 Pa · s/m$^2$ and the thickness of the absorber being 20 mm and 40 mm.

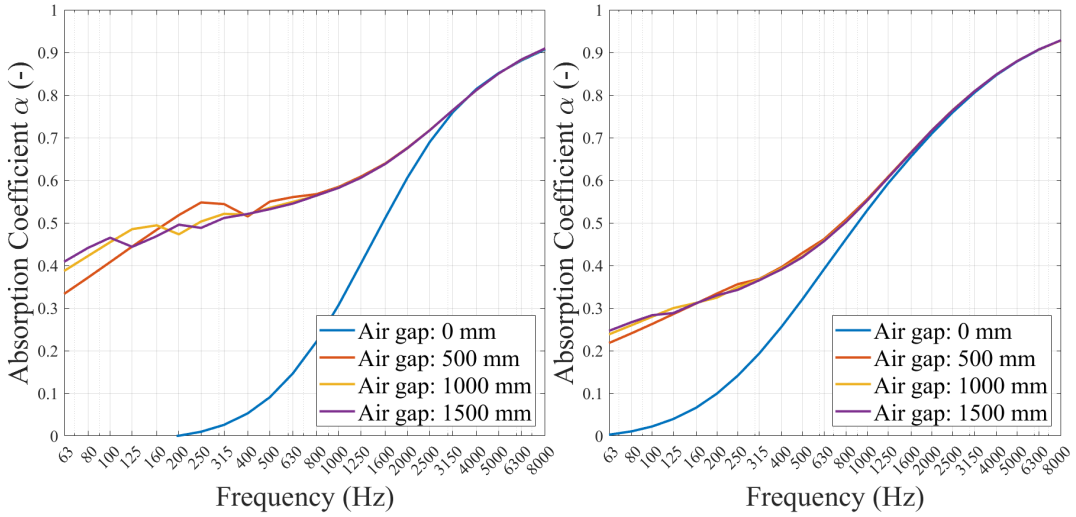


**(a)** Thickness of the absorber: 20 mm

**(b)** Thickness of the absorber: 40 mm

**Figure 4.9:** The two figures compare the absorption coefficient as a function of frequency for different air gap, and for two absorber thicknesses. The airflow resistivity is fixed at 104 690 Pa · s/m$^2$ in both cases.

In Figure 4.9, there are almost no peaks in the lower frequencies for the thinner absorber, and for the thicker absorbers, all the curves for all three air gaps are nearly aligned, unlike in Figures 4.7 and 4.8 where some variation was observed. Increasing the thickness of the absorber still improves the absorption at higher frequencies, same as for the other airflow resistivity in Figure 4.6, 4.7 and 4.8. The absorber without an air gap follows a similar trend as the previous figures and improves the absorption over all frequencies with a thicker absorber.

Figure 4.10 show the relationship between absorption coefficient, airflow resistivity.

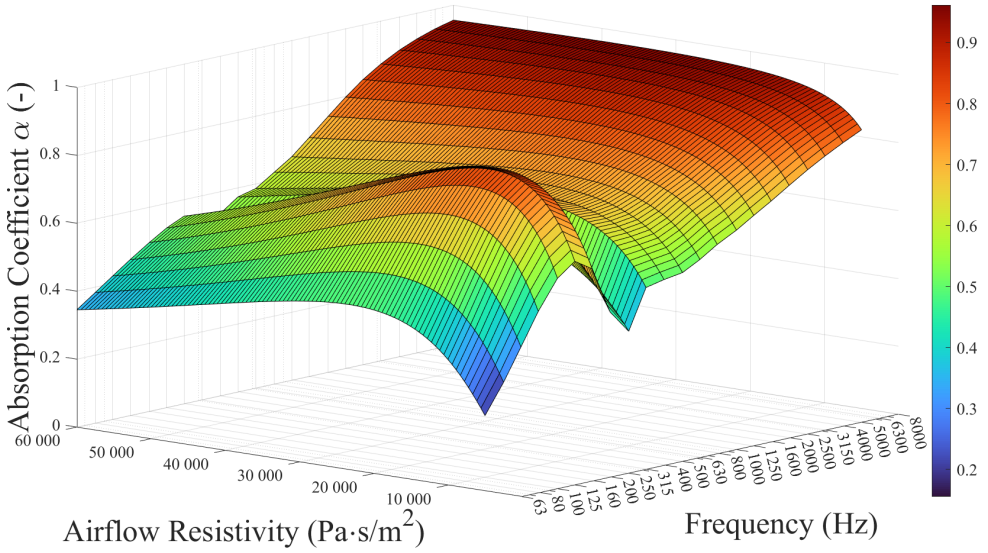


**Figure 4.10:** 3D plot illustrating the relationship between absorption coefficient, airflow resistivity, and frequency for an absorber with the thickness 40 mm and an air gap of 500 mm.

Figure 4.10 shows that at higher frequencies, the absorption coefficient exceeds 0.8 for most airflow resistivities, indicating that the material absorbs higher frequencies quite effectively. For lower frequencies, below 500 HZ, the figure shows that the absorption can be maximized for lower airflow resistivities and reaches its maximum effect around 15 000 $\mathrm{Pa} \cdot \mathrm{s/m^2}$.

# 5

# Discussion

*This chapter aims to analyze and interpret the results presented in the previous section. In addition to discussing the findings, it addresses the uncertainties and limitations of the study, exploring the reliability of the results. The discussion will also cover potential adaptations of the model and construction, along with suggestions for future work and improvements in measurement methods.*

## 5.1 Evaluation of the Validation

The validation results align well with the Norflag simulation and the developed model up to approximately 800 Hz, as seen in Figure 4.5. Beyond this frequency, a discrepancy emerges, with Norflag values generally exceeding those of the developed model. Although no definitive cause has been identified for this divergence, it may be valuable in future work to investigate possible contributing factors, such as model limitations or frequency-dependent behaviors not accounted for in Norflag's parameters.

Room measurements, however, did not align as closely with either Norflag or the developed model. The results in Figure 4.1 show a decline in the absorption coefficient above 800 Hz, potentially linked to the surface characteristics of the tiles or the formation of standing waves, suggesting that the room's sound field may not have achieved the necessary diffuseness. Given the room's Schroeder frequency of approximately 300 Hz, it is likely that measurements taken below this frequency are subject to increased uncertainty due to a non-diffuse sound field, impacting reliability. Future work could focus on refining room measurement techniques or introducing corrective factors for environments where diffuse field assumptions are not fully met.

The validation results indicate that the model is not entirely perfect, particularly at higher frequencies where deviations between the model and Norflag are more noticeable. However, the strong alignment between simulated and measured results at lower frequencies suggests that the model can still provide reliable evaluations within this range.

## 5.2 Evaluation of the Simulations

In all the figures in Section 4.2, it is clear that the presence of an air gap enhances the absorption coefficient, particularly at lower and mid-range frequencies. A critical point is observed around 800 Hz, where the impact of the air gap begins to diminish. At higher frequencies, the air gaps provide no additional benefit, and the absorption curves for absorbers with and without air gaps converge. This improvement in absorption is primarily due to the increased path length and longer interaction time that sound waves experience when there is an air gap behind the absorber. Additionally, the air cavity allows for resonance effects, where sound waves resonate within the gap and are subsequently absorbed by the material.

The critical point at 800 Hz marks the threshold beyond which the size of the air gap no longer contributes to improved absorption—at this stage, the cavity's presence is sufficient to enhance the absorber's performance. At lower frequencies, a distinct absorption peak is observed for all three air gaps. According to the quarter-wavelength theory, the particle velocity reaches its maximum at one-quarter of a wavelength from a reflective surface, which optimizes sound absorption, and the reflected wave from the backing cancels the incoming wave.

Figure 5.1 illustrates the targeted quarter-wavelength zones for the results shown in Figure 4.7a. The quarter-wavelength for each air gap is calculated using Equation 2.1, with the corresponding frequencies indicated by the dotted lines.

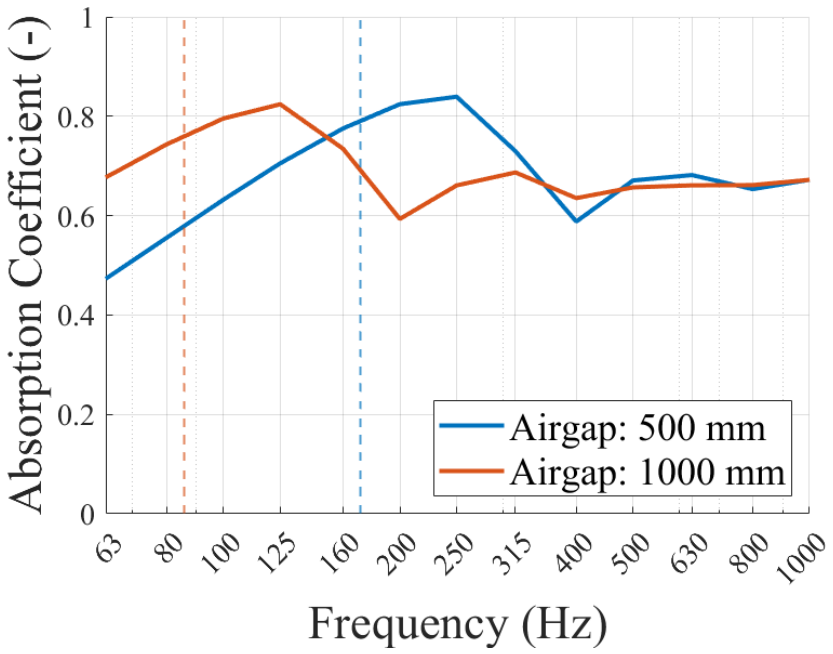


**Figure 5.1:** Targeted quarter-wavelength zones for two air gaps for a 20 mm thick absorber with airflow resistivity set to 39 260 Pa · s/m$^2$.

For example, with a 0.5 m air gap, the quarter-wavelength theory predicts a peak

absorption at around 170 Hz. However, the simulation shows that the actual peak occurs at 250 Hz, and the peak from the measurements (Figure 4.1) occurs at approximately 200 Hz. This shift between the theoretical predictions and the actual peak suggests that more factors, such as material properties and room acoustics, affect the absorption performance.

In general, increasing the thickness of the absorber enhances absorption at higher frequencies. This is because thicker material provides a longer path for sound waves to travel, allowing for greater energy dissipation through internal friction and momentum loss, which often benefits higher frequencies with shorter wavelengths, the most from this increased interaction with the absorber.

However, at lower frequencies, as shown in Figures 4.7, 4.8, and 4.9, increasing the thickness from 20 mm to 40 mm leads to a decrease in absorption for all three air cavities. Interestingly, this trend is not observed when the absorber is mounted directly on a rigid backing, where increasing thickness improves absorption over all frequencies. This suggests that the interaction between the absorber and the air cavity is a critical factor, with higher airflow resistivity playing a significant role in these results.

Materials with higher airflow resistivity, which are denser or more compact, resist air movement through their pores. At low frequencies, the airflow resistivity prevents sound waves from penetrating deeply into the material, causing them to reflect rather than be absorbed. As a result, thicker absorbers with high airflow resistivity reflect more sound at low frequencies, diminishing their absorption efficiency. In contrast, thinner absorbers with lower resistivity allow sound waves to pass through more effectively, enabling better interaction with the air cavity and having a better resonance effect.

Figure 4.6 demonstrates this phenomenon, showing that an absorber with a lower airflow resistivity of 10,900 Pa $\cdot$ s/m$^2$ exhibits improved absorption across all frequencies, even when the thickness is increased. Figure 4.10 shows a 3D model of the absorption coefficient over frequencies and airflow resistivity.

As shown in Figure 4.10, the absorption coefficient reaches its maximum effect for lower frequencies at an airflow resistivity of approximately 15 000 Pa $\cdot$ s/m$^2$ for a 40 mm thick absorber, after which it begins to decrease. This indicates that optimizing both thickness and airflow resistivity is crucial for maximizing absorption in the lower frequencies, mainly when large air cavities are present.

## 5.3 Uncertintes and limitaions

The model developed in this study only calculates assuming an infinite area, which never happens in a real-world scenario. As a result, the model's results cannot be directly applied to real-world situations without further consideration. In practical applications, ceiling absorbers have finite dimensions, leading to additional effects such as edge diffraction, reflections from walls, and conjunctions, which the model

does not account for. A more discussion on finite-area considerations and alternative calculation methods is provided in Section 5.4.

The simulations were conducted using the Delany-Bazley impedance model, one of the most widely used models for porous absorbers due to its simplicity and ease of adaptation to diffuse field calculations. However, the DB model is limited because it is based on empirical measurements and only incorporates basic material properties, such as thickness and airflow resistivity. Other models, such as the one proposed by Mechel [33], also factor in porosity, providing a more comprehensive characterization of the material.

More accurate models, such as the one developed by Allard [31], account for dynamic properties like the inertial and viscous forces of air within the material and the dynamic bulk modulus, which considers molecular displacement under pressure. These additional parameters improve accuracy but also increase the complexity of the calculations, especially when adapting the model for diffuse field scenarios [31]. While more advanced models, such as Allard, provide greater precision, they also require detailed material data and more computational effort, which were beyond the scope of this study.

### 5.3.1 Measurements

The measurement environment also posed certain limitations. The Schroeder frequency, calculated as $f_s = 2000 \cdot \sqrt{T/V}$, was approximately 300 Hz for the room used in this study. This means that results below this frequency are uncertain due to the room's modal behavior. Furthermore, the measured absorption coefficient (Figure 4.1) shows a noticeable decay starting around 1000 Hz. The same decay is not observed in the tube measurements (Figure 4.2), suggesting that the decay from the room measurement may be caused by room acoustics rather than the material properties of the absorber itself. The absence of furniture, diffusers, and the presence of a carpet may have contributed to standing waves and other acoustic interferences, particularly at higher frequencies. Additionally, the values may have been influenced by a poor signal-to-noise ratio. Unfortunately, the analyzer used in the measurements did not provide data on the signal-to-noise ratio.

The tube method employed in this study has limitations regarding the frequency range. The lower frequency limit is around 200 Hz, and the upper limit is 2000 Hz, which affects the accuracy of the airflow resistivity calculations. These frequency constraints introduce uncertainties in low- and high-frequency measurements, limiting the precision of the airflow resistivity estimates. As a result, while the tube method provides valuable insights, it is not without its limitations when applied to the wide frequency range typically encountered in practical scenarios.

## 5.4 Finite Area and Edge Effect

A significant limitation of this study's model is its assumption of infinite areas, which does not reflect real-world conditions. In practical applications, absorbers

have finite dimensions

One approach to account for finite areas is the Thomasson equation, which is used in Norflag and adjusts for the edge effect. The Thomasson equation compensates for the additional absorption caused by sound waves diffracting at the edges of the absorber during reverberation room measurements. However, this correction still may not accurately represent the performance of absorbers in real-world applications, such as suspended ceilings. In practice, ceiling absorbers are often mounted against walls, eliminating the free edges that allow sound to diffract. This means that the higher absorption values measured in a reverberation room due to edge effects may not translate to real-world scenarios. Despite these challenges, reverberation room measurements remain the primary method for classifying ceiling absorbers.

For example, Ecophon's Master A [42] ceiling tile—40 mm thick with an airflow resistivity of 39,620 Pa $\cdot$ s/m$^2$ is one commonly used ceiling tile. According to the supplier, the absorption coefficient for the 400 mm air gap remains close to ideal (nearly $\alpha = 1$) from 250 Hz and above. The results from this study's model are further below the supplier's data, suggesting that the edge effect in the reverberation room setup can inflate absorption values and that the finite size has some advantages.

## 5.5 Challenges for Building Acousticans

A additional issue identified in this study is the treatment of room volume and ceiling height, particularly when assessing the impact of suspended ceilings. According to ISO 3382-2 [27], the height is measured up to the suspended ceiling. However, during the validation measurement, significant contrasts occurred when comparing conditions with and without the ceiling. The volume above the ceiling accounted for 19 % of the total room volume without the suspended ceiling, leading to different results depending on which volume was used in the calculation.

ISO354 does not allow for the volume to change in the calculation, but de Godoy and Barry [1] discuss how allowing different volumes can lead to different results. Future investigations should explore the threshold at which changes in room volume become significant and how these volume changes should be accounted for in acoustic models. Another area for further study involves the interaction between the air above the ceiling and the absorber, particularly in cases where large volumes of air may behave as a separate acoustic space rather than a simple air gap.

Future research could address the discrepancies between measurement standards for sound absorption, particularly the use of octave bands in SS 25268 [4] and NS 8195 [5] versus the third-octave band requirement in the tube and reverberation room methods [8, 6, 7] and for verifications [27]. The conversion process from third-octave to octave bands, as defined in ISO 11654 [43], introduces practical absorption coefficients $\alpha_p$, but this transformation may introduce rounding and

averaging effects that impact measurement precision.

Further investigation is needed to determine how these band differences affect acoustic evaluations. Additionally, with new requirements in SS 25268 for office and hospital ceilings, there is a need for methods to verify compliance beyond relying solely on supplier data. The existing methods for building verification do not specifically measure sound absorption in specific areas. Accurate in-situ measurement techniques would allow for real-time validation of the acoustic performance of ceiling absorbers and improve practical assessments in real-world environments.

## 5.6 Furture Research

While the current study successfully developed a simplified model to simulate the absorption characteristics of porous ceiling absorbers with large cavities, several areas warrant further exploration. As the thesis work progressed, it became clear that more research on the area and the standards used today need to be explored and questioned. Here follows a list of topics that could be interesting to investigate further in the future:

- The current model assumes infinite areas for the ceiling absorbers, which do not accurately reflect real-world installations. Future work should focus on adapting the model to account for finite areas, which would provide a more precise prediction of absorption performance. Also implementing more advanced acoustocal impedance models, such as those by Allard, could improve the accuracy of predictions, especially for absorbers with complex materials and large air gaps.
- Future research should aim to validate the model with experimental measurements taken from more room types and installation settings. Testing different room sizes, measurement methods, materials, and absorber configurations would help generalize the findings and increase confidence in the model's applicability.
- Further research could investigate how varying material properties, such as airflow resistivity and porosity, interact with mounting conditions and air cavity sizes. More research is also needed on the edge effect and its impact on the classification system for ceiling absorbers.
- One limitation of current measurement methods is their inability to precisely measure absorption coefficients on-site. Accurate in-situ measurement techniques would allow for real-time validation of the acoustic performance of ceiling absorbers and improve practical assessments in real-world environments.

# 6

# Conclusion

This thesis explored the predictability of porous ceiling absorbers with large cavities by developing a simulation model based on the transfer matrix method and the Delany-Bazley impedance model. The findings show that large air gaps have a significant impact on the absorption characteristics of ceiling absorbers, particularly at low and mid-range frequencies. However, the impact of an air cavity diminishes at higher frequencies. While increasing the thickness of absorbers generally improves absorption at higher frequencies, it does not always enhance performance at lower frequencies, especially when airflow resistivity is high. In fact, thicker absorbers can sometimes reduce low-frequency absorption.

This study's model is limited to calculating infinite area, but that limitation opens up for discussion regarding the pros and cons of calculating with the edge effect and the different mounting conditions in reverberation rooms and on-site measurements.

Overall, this thesis contributes to a better understanding of how large air cavities and absorber properties influence room acoustics. The results provide valuable insights for building acousticians and open up the topic of standards, reverberation room measurement, and on-site measurement regarding ceiling systems in modern buildings. The results and discussion lay the groundwork for future research in acoustic modeling, connecting the gap between theoretical simulations and practical applications in real-world construction.

# Bibliography


[1] M. de Godoy and P. J. Barry, "A study of the influence of mounting conditions on the measured sound absorption in laboratory tests of suspended ceilings," *The Journal of the Acoustical Society of America*, vol. 119, no. 1, pp. 33–36, jan 2006, doi:10.1121/1.2139076.

[2] C. H. Jeong, "Sabine absorption coefficient predictions using different radiation impedances of a finite absorber," *Acta Acustica united with Acustica*, vol. 101, no. 4, pp. 663–667, July 2015, doi:10.3813/AAA.918861.

[3] M. L. S. Vercammen, "Improving the accuracy of sound absorption measurement according to ISO 354," in *Proceedings of the International Symposium on Room Acoustics*. Melbourne, Australia, 2010.

[4] *Building acoustics - Sound requirements for spaces in buildings - Healthcare premises, rooms for education, preschools and leisure-time centres, rooms for office work, hotels, and restaurants*, SS 25268:2023, Swedish Institution for Standards, Stockholm, Sweden, 2023.

[5] *Acoustic conditions in buildings - Sound classification of various types of buildings*, NS 8175:2012, Standrad Norge, Norway, 2019.

[6] *Acoustics - Determination of sound absorption coefficient and impedance in impedances tubes - Part 1: Method using standing wave ratio*, SS EN-ISO 10534-1:1996, European Committee for Standardization, 2001.

[7] *Acoustics-Determination of acoustic properties in impedance tubes - Part 2: Two-microphone technique for normal sound absorption coefficient and normal surface impedance*, SS EN-ISO 10534-2:2023, European Committee for Standardization, 2023.

[8] *Acoustics - Measurement of sound absorption in a reverberation room*, SS EN-ISO 354:2003, European Committee for Standardization, 2003.

[9] A. Farina and A. Torelli, "Measurement of the sound absorption coefficient of materials with a new sound intensity technique," *Journal of The Audio Engineering Society*, March 1997.

[10] Folkhälsomyndigheten, "Hälsoeffekter av buller och höga ljudnivåer," 2019,

[Online]. Available:
https://www.folkhalsomyndigheten.se/publikationer-och-material/publikationsarkiv/h/halsoeffekter-av-buller-och-hoga-ljudnivaer/?pub=60532 (accessed on: 2024-06-15).

[11] T. E. Vigran, *Building Acoustics*. London, England: CRC Press, 2014.

[12] M. Kleiner, *Acoustics and Audio Technology*, 3rd ed. USA: J. Ross Publishing, 2012.

[13] M. Long, *Architectural Acoustics*, 2nd ed. Amsterdam, Netherlands: Elsevier Science & Technology, 2014.

[14] L. E. Kinsler, *Fundamentals of Acoustics*, 4th ed. New York, USA: John Wiley & Sons, 2000.

[15] H. Kuttruff, *Room Acoustics*, 6th ed. Boca Raton, FI, USA: CRC Press, 2016.

[16] Arbetsmiljöverket, "About us," 2024, [Online]. Available: https://www.av.se/en/about-us/ (accessed on: 2024-06-12).

[17] *Arbetsmiljöverkets föreskrifter om buller samt allmänna råd om tillämpningen av föreskrifterna*, AFS 2005:16, Arbetsmiljöverket, Stockholm, Sweden, 2010. [Online]. Available: https://www.av.se/arbetsmiljoarbete-och-inspektioner/publikationer/foreskrifter/buller-afs-200516/ (accessed on: 2024-06-14).

[18] Swedish Institute for Standards, "Organisation," 2024, [Online]. Available: https://www.sis.se/en/about_sis/sisorganisation/ (accessed on: 2024-06-14).

[19] Swedish Institute for Standard, "Hur tas en standard fram?" 2024, [Online]. Available: https://www.sis.se/standardutveckling/delta-i-standardutveckling/hur-gar-arbetet-till/ (accessed on: 2024-06-14).

[20] Arbeidstilsynet, "About us," 2024, [Online]. Available: https://www.arbeidstilsynet.no/en/about-us/ (accessed on: 2024-06-12).

[21] *Act relating to the working environment, working hours and employment protection, etc. (Working Environment Act)*, Ministry of Labour and Social Inclusion, Norway, 2023.

[22] Standard Norge, "Om oss," 2024, [Online]. Available: https://standard.no/om-oss/ (accessed on: 2024-06-15).

[23] StandardNorge, "Lydklasse," [Online]. Available: https://standard.no/fagomrader/akustikk-og-stoy/lydklasser/ (accessed on: 2024-10-21).

[24] Standard Norge, "Kapittel 13 inneklima og helse - referansestandarder til byggteknisk forskrift tek17 med veiledning." [Online]. Available: https://standard.no/nettbutikk/standarder-for-byggfag/

referansestandarder-til-byggteknisk-forskrift-tek-med-veiledning/kapittel-13-inneklima-og-helse/ (accessed on: 2024-10-21).

[25] H. Høilund-Kaupang, "Bruk av lydabsorbenter i bygninger: Prinsipper og datasamling," *SINTEF Byggforsk kunnskapssystemer. Byggforskserien*, no. 543.414, Oct. 2014.

[26] A. Nowoświat, "Impact of Temperature and Relative Humidity on Reverberation Time in a Reverberation Room," *Buildings*, vol. 12, no. 8, Aug. 2022, doi:10.3390/buildings12081282.

[27] *Acoustics - Measurement of room acoustic parameters - Part 2: Reverberation time in ordinary rooms*, SS-EN ISO 3382-2:2008, European Committee for Standardization, 2008.

[28] M. Waaranperä and J. Forssén, "Time-domain model for spherical wave reflection in a flat surface with absorber character – application to the sopra measurement method," *Applied Acoustics*, vol. 227, 2025, doi:10.1016/j.apacoust.2024.110251.

[29] H. Peperkamp and M. Vercammen, "Thermally activated concrete slabs and suspended ceilings," in *Proceedings of the International Conference on Acoustics (NAG/DAGA)*. Rotterdam, Netherlands, 2009.

[30] M. E. Delany and E. N. Bazley, "Acoustical properties of fibrous absorbent materials," *Applied Acoustics*, vol. 3, no. 2, Aug. 1970, doi:10.1016/0003-682X(70)90031-9.

[31] D. Oliva and V. Hongisto, "Sound absorption of porous materials – accuracy of prediction methods," *Applied Acoustics*, vol. 74, no. 12, pp. 1473–1479, July 2013, doi:10.1016/j.apacoust.2013.06.004.

[32] Y. Miki, "Acoustical properties of porous materials - Modifications of Delany-Bazley models," *Journal of the Acoustical Society of Japan*, vol. 11, no. 1, pp. 19–24, March 1990, doi:10.1250/ast.11.19.

[33] F. P. Mechel, "Design charts for sound absorber layers," *The Journal of the Acoustical Society of America*, vol. 83, no. 3, pp. 1002–1013, March 1988, doi:10.1121/1.396045.

[34] S.-I. Thomasson, "On the Absorption Coefficient," *Acustica*, vol. 44, pp. 265–273, 1980.

[35] P. Gerlee and T. Lundh, *Vetenskapliga modeller: Svarta lådor, röda atomer och vita lögner*. Lund, Sweden: Studentlitteratur, 2012.

[36] K. Säfsten and M. Gustavsson, *Research methodology: For engineers and other problem-solvers 2.0*, 2nd ed. Lund, Sweden: Studentlitteratur, 2024.

[37] Mathworks, "MATLAB," [Online]. Available:

https://se.mathworks.com/products/matlab.html (accessed on: 2024-09-19).

[38] Norsonic, "NORFlag Acoustic Performance Estimation Software," [Online]. Available: https://www.norsonic.asia/product/norflag-acoustic-performance-estimation-software/ (accessed on: 2024-09-19).

[39] T. E. Vigran, *Manual for WinFLAG, version 2.4*, Trondheim, Norway, 2011.

[40] Norsonic, "Sound level meters - Nor140 Sound analyser," [Online]. Available: https://www.norsonic.com/products/sound-level-meters/nor140-sound-analyser/ (accessed on: 2024-09-23).

[41] Head acoustics, "Squadriga iii – standard system for mobile sound and vibration measurement," [Online]. Available: https://www.head-acoustics.com/products/data-acquisition/squadriga-iii (accessed on: 2024-10-06).

[42] Ecophon, "Ecophon Master A," [Online]. Available: https://www.ecophon.com/sv/produkter/modular-ceilings/master/master-a/ (accessed on: 2024-10-15).

[43] *Acoustics - Sound absorbers for use in buildings - Rating of sound absorption*, SS EN-ISO 11654:1997), European Committee for Standardization, 1997.

**DEPARTMENT OF ARCHITECTURE OF CIVIL ENGINEERING**
**CHALMERS UNIVERSITY OF TECHNOLOGY**
Gothenburg, Sweden
www.chalmers.se


CHALMERS
UNIVERSITY OF TECHNOLOGY